Received: 11 August 2023 | Accepted: 27 November 2023

DOI: 10.1111/1462-2920.16556

RESEARCH ARTICLE

ENVIRONMENTAL MICROBIOLOGY Applied Microbiology International

Protistan community composition and metabolism in the North Pacific Subtropical Gyre: Influences of mesoscale eddies and depth

Samantha J. Gleich[1] | **Sarah K. Hu**[2] | **Arianna I. Krinos**[3,4,5] | **David A. Caron**[1]

[1]Department of Biological Sciences, University of Southern California, Los Angeles, California, USA

[2]Department of Oceanography, Texas A&M University, College Station, Texas, USA

[3]MIT-WHOI Joint Program in Oceanography and Applied Ocean Science and Engineering, Cambridge and Woods Hole, Cambridge, Massachusetts, USA

[4]Department of Biology, Woods Hole Oceanographic Institution, Woods Hole, Massachusetts, USA

[5]Department of Earth, Atmospheric, and Planetary Science, Massachusetts Institute of Technology, Cambridge, Massachusetts, USA

Correspondence
Samantha J. Gleich, Department of Biological Sciences, University of Southern California, Los Angeles, CA, USA.
Email: gleich@usc.edu

Funding information
Department of Energy Computational Science Graduate Fellowship, Grant/Award Number: DE-SC0020347; NSF Award, Grant/Award Number: OCE-2327203; Simons Collaboration on Ocean Processes and Ecology, Grant/Award Number: P49802; The Simons Collaboration on Computational Biogeochemical Modeling of Marine Ecosystems (CBIOMES), Grant/Award Number: 549931

Abstract

Marine protists and their metabolic activities are intricately tied to the cycling of nutrients and the flow of energy through microbial food webs. Physiochemical changes in the environment, such as those that result from mesoscale eddies, may impact protistan communities, but the effects that such changes have on protists are poorly known. A metatranscriptomic study was conducted to investigate how eddies affected protists at adjacent cyclonic and anticyclonic eddy sites in the oligotrophic ocean at four depths from 25 to 250 m. Eddy polarity impacted protists at all depths sampled, although the effects of eddy polarity were secondary to the impact of depth across the depth range. Eddy-induced vertical shifts in the water column yielded differences in the cyclonic and anticyclonic eddy protistan communities, and these differences were the most pronounced at and just below the deep chlorophyll maximum. An analysis of transcripts associated with protistan nutritional physiology at 150 m revealed that cyclonic eddies may support a more heterotrophic community, while anticyclonic eddies promote a more phototrophic community. The results of this study indicate that eddies alter the metabolism of protists particularly in the lower euphotic zone and may therefore impact carbon export from the euphotic zone.

INTRODUCTION

Mesoscale eddies are common physical features in marine environments that may lead to notable changes in oceanic biogeochemistry. Cyclonic eddies are associated with a negative sea level anomaly (SLA), an uplift of isopycnal surfaces, and upwelling of inorganic nutrients from deep waters to the deep chlorophyll maximum (DCM) and lower euphotic zone (Barone et al., 2019, 2022; Benitez-Nelson et al., 2007; Cornec et al., 2021; McGillicuddy et al., 1998; Xiu & Chai, 2020). Conversely, anticyclonic eddies are associated with a positive SLA, a deepening of isopycnal surfaces, and low inorganic nutrient availability at and below the DCM (Barone et al., 2019, 2022; Cornec et al., 2021; McGillicuddy, 2016; Xiu & Chai, 2020). Both cyclonic and anticyclonic eddies have the potential to physically isolate populations of microorganisms by trapping and transporting water masses, which may result in eddy communities that differ taxonomically and

metabolically from those of surrounding waters (Bracco et al., 2000; Chelton et al., 2011; McGillicuddy, 2016; Venkatachalam et al., 2017). Additionally, mesoscale eddies can vertically displace water layers, which can alter the depth distribution of microorganisms in the water column (Nelson et al., 2014; Rii et al., 2022). The physiochemical changes that result from the vertical displacement of waters also have the potential to impact microbial community dynamics (Brown et al., 2008; Dugenne et al., 2023; Harke et al., 2021). Cyclonic eddies are thought to be particularly important in oligotrophic ocean environments, as cyclone-induced physical forcing has been associated with elevated phytoplankton biomass and primary production (Benitez-Nelson et al., 2007; Bidigare et al., 2003; Falkowski et al., 1991; Karl, 1999; Letelier et al., 2000; McGillicuddy et al., 1998; Rii et al., 2008). The specific effects that these mesoscale physical features have on microbial community composition and metabolism are therefore critical in understanding the cycling and vertical flux of organic carbon in oligotrophic ocean systems.

The trophic activities of protists in relation to mesoscale physical forcing are important to consider when evaluating the impact that eddies have on carbon cycling, given the major roles that protists play as primary producers and consumers in marine waters (Calbet & Landry, 2004; Caron et al., 2012; Stoecker et al., 2017). Previous studies have demonstrated that rates of primary production and grazing may be altered inside eddy centres and that the impacts that eddies have on these processes may vary by depth (Landry et al., 2008; Paterson et al., 2007). Specifically, a study carried out in the North Pacific Subtropical Gyre (NPSG) by Landry et al. (2008) documented higher rates of primary production near the DCM of a cyclonic eddy relative to a region outside of the eddy. The higher primary production rates inside of the cyclonic eddy at this depth were also associated with higher grazing rates by microzooplankton from the DCM to ≈30 m below the DCM in the eddy centre (Landry et al., 2008).

Transcriptomic and metatranscriptomic sequencing efforts have augmented field studies investigating the composition, standing stocks, and trophic activities of protists in recent years. Such studies have expanded our ability to characterize shifts in the nutritional physiology of marine protists as they relate to environmental parameters such as light, depth, nutrients, and so on (Cohen et al., 2021; Hu et al., 2018; Lambert et al., 2022; Lie et al., 2017). Phototrophic metabolism, for example, is recognizable in protistan transcriptomic data because photosynthetic pathways are well-studied and highly conserved across taxonomic groups (Becker et al., 2021; Worden et al., 2015). Pathways involved in protistan heterotrophic metabolism are less well-described, but some recent studies have begun to characterize heterotrophic metabolism using transcriptomic and proteomic approaches (Burns et al., 2018; Koppelle et al., 2022; Labarre et al., 2020; Lambert et al., 2022; McKie-Krisberg et al., 2018; Obiol et al., 2023; Rubin et al., 2019; Yutin et al., 2009). Culture-based transcriptomic studies have aided our ability to identify specific proteins and pathways that may be associated with grazing processes in protists. For example, a study carried out by Massana et al. (2021) documented increases in the expression of cytoskeletal, protein folding, and proton pump-related genes when *Cafeteria burkhardae*, a heterotrophic nanoflagellate, was actively grazing on bacterial prey. Other transcriptomic studies carried out by Liu et al. (2015, 2016) documented increases in the expression of genes associated with fatty acid metabolism when mixotrophic prymnesiophytes and chrysophytes shifted to a primarily heterotrophic lifestyle. These culture-based studies, among others, identified potential heterotrophy biomarker genes that have been used in field investigations to explore shifts in the metabolism of protists using metatranscriptomic approaches (Cohen et al., 2021; Hu et al., 2018; Labarre et al., 2020; Lambert et al., 2022).

A eukaryotic metatranscriptomic study was carried out on samples collected from cyclonic and anticyclonic eddy centres at four depths (25 m, DCM, 150 m, and 250 m) in the NPSG to determine how mesoscale physical forcing and depth impacted protistan community diversity and metabolism in the euphotic and upper mesopelagic waters of the oligotrophic ocean. The results of this study revealed that the displacement of waters that occurred due to mesoscale eddy activity altered the vertical distribution of protistan communities and their resulting physiologies. These effects of mesoscale eddy activity on protistan community composition and physiology were particularly pronounced at 150 m depth. Eddy polarity influenced how similar protistan communities at 150 m depth were to euphotic zone communities, and in turn, altered the relative importance of phototrophy in the nutritional physiology of the protistan communities. An analysis of transcripts that may be associated with the nutritional physiology of protists revealed that transcripts associated with phototrophic metabolism were found at higher relative abundances at 150 m in the anticyclone, while transcripts that may be associated with heterotrophic metabolism were found at higher relative abundances at 150 m in the cyclone. The results obtained from this study highlight that mesoscale eddies can shift the depth at which metabolic processes occur in the water column and can in turn alter the biogeochemical cycling of organic carbon in the upper ocean.

EXPERIMENTAL PROCEDURES

Sample collection

Samples used for the eukaryotic metatranscriptomic study were collected during the Simons Collaboration

on Ocean Processes and Ecology (SCOPE) FALKOR cruise that took place in March and April 2018 near Station ALOHA (A Long-term Oligotrophic Habitat Assessment; 22°45′ N, 158°00′ W) in the NPSG. The movement and progression of the sampled eddy dipole (Figure 1A) were tracked before, during, and after the cruise by identifying the location of the minimum and maximum corrected SLA inside of the cyclonic and anticyclonic eddies respectively. Seawater samples for metatranscriptomics were collected during the cruise at a site inside the cyclonic eddy on 4 April 2018, and a site inside the adjacent anticyclonic eddy on 8 April 2018. Triplicate samples were collected at each eddy site at 25 m, the depth of the DCM (112 m cyclone; 122 m anticyclone), 150 m, and 250 m using a Niskin bottle rosette sampler. The 150 m sampling depth has been characterized as the base of the euphotic zone at Station ALOHA and has been used as a reference depth for calculating vertical carbon flux in this region (Karl et al., 1996). For each metatranscriptomic sample, 12–18 L of seawater was filtered onto a 0.7 μm GF/F filter (Table S1). The filters were preserved in RNALater, flash-frozen in liquid nitrogen, and stored at −80°C until total RNA was extracted.

Environmental data were collected at the cyclonic and anticyclonic eddy sampling sites and at a non-eddy (i.e., SLA ≈ 0) site during the cruise. Vertical profiles of potential density, chlorophyll fluorescence, temperature, and oxygen concentration were obtained using a Sea-Bird SBE 911 plus CTD (Sea-Bird, Bellevue, WA) at each site. On the CTD, a Wet Labs ECO-FLNTU fluorometer was used to measure chlorophyll fluorescence, and a Sea-Bird SBE 43 sensor was used to measure oxygen concentration. CTD data were processed following the standard protocols used for the Hawaii Ocean Time series (https://hahana.soest.hawaii.edu/hot/protocols/). Samples were collected for measurements of inorganic nutrient concentrations, total organic carbon (TOC) concentrations, and cell abundances (via flow cytometry) near each eddy site 2 days before metatranscriptome sample collection (2 April 2018, in the cyclone; 6 April 2018, in the anticyclone). Concentrations of $NO_3^- + NO_2^-$ and PO_4^{3-} were quantified at the University of Hawaii as described by Armstrong et al. (1967) and Murphy and Riley (1962), respectively. Total organic carbon concentrations were measured as described by Wear et al. (2020). Samples were collected for flow cytometry by preserving seawater in 16% paraformaldehyde at a final concentration of 0.24% and were run on an InFlux Flow cytometer (BD, Franklin Lakes, NJ) at the University of Hawaii at Manoa to quantify the abundances of *Prochlorococcus*, *Synechococcus*, heterotrophic bacteria, and picoeukaryotes at various depths in the cyclonic and anticyclonic eddy centres according to Monger and Landry (1993).

RNA extraction, library preparation, and sequencing

Total RNA was extracted from the filters using the Qiagen RNeasy Mini Kit (Qiagen, Valencia, CA, no. 74106). The RNALater was removed from the preserved filters by pipetting the liquid out of the sample tubes. Then, 1.5 mL of Buffer RLT and 0.5 mm silica beads were added directly to the tubes and the tubes

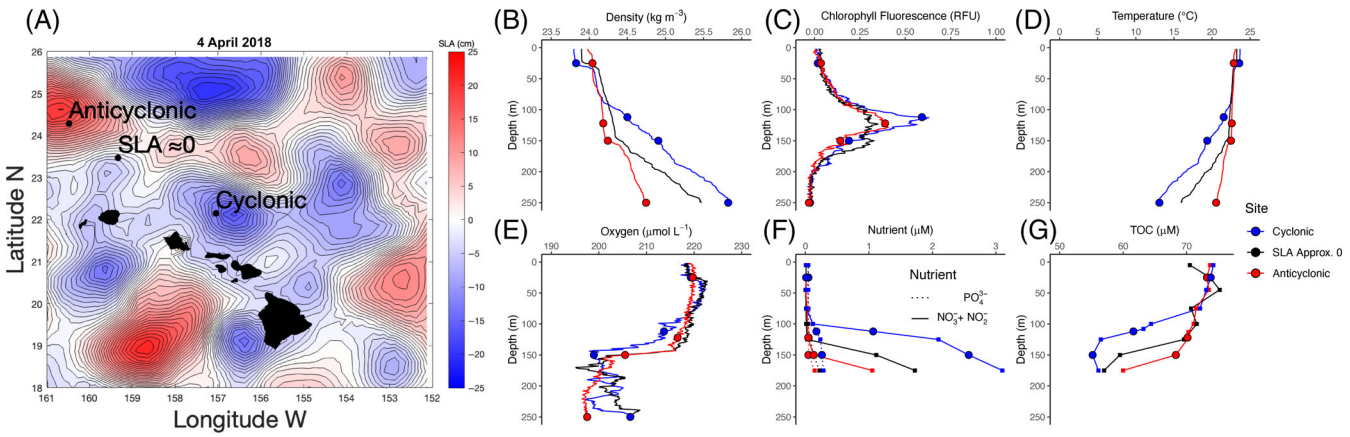

FIGURE 1 Environmental parameters observed at the cyclonic and anticyclonic eddy sampling sites during the 2018 FALKOR cruise. Panel A shows a map of the corrected (as per Barone et al., 2019) sea level anomaly measurements on the day that the cyclonic eddy metatranscriptomic samples were collected (4 April 2018). The anticyclonic eddy metatranscriptomic samples were collected 4 days after the cyclonic eddy samples (8 April 2018). The SLA data were obtained from the Copernicus Marine Service. The physiochemical data collected at the non-eddy site (i.e., SLA ≈ 0) were used to visualize differences in the physiochemistry at the eddy sites relative to ambient waters. Metatranscriptomic samples were not collected at this non-eddy site. The black dots on the map show the specific sampling locations within each eddy. Panels B–G show the potential density (CTD), chlorophyll fluorescence (CTD), temperature (CTD), oxygen (CTD), inorganic nutrients ($NO_3^- + NO_2^-$ and PO_4^{3-}), and total organic carbon (TOC) profiles at the cyclonic and anticyclonic eddy sampling sites. The circles on the depth profiles in panels B–G denote the depths at which metatranscriptome samples were collected.

were vortexed for 6 min to lyse the filtered cells before RNA extraction. An on-column DNase digestion step was carried out using the Qiagen RNase-free DNase digestion kit (Qiagen, Valencia, CA, no. 79256) to remove any genomic DNA contamination. After extraction, the concentration of RNA in each sample was quantified using a Qubit 2.0 (ThermoFisher, Waltham, MA, no. Q32866). The extracted RNA was quality-checked on an Agilent BioAnalyzer (Agilent Technologies, Santa Clara, CA) at the University of Southern California Genome Core. Before library preparation, RNA concentrations were normalized and ERCC spike-in mix (ThermoFisher, Waltham, MA, no. 4456740), an internal RNA standard, was added to each sample. Library preparation was carried out at the University of Southern California Genome Core using the Kapa mRNA HyperPrep kit (Kapa Biosystems, Inc., Wilmington, MA, no. KK8504), which included a poly-A tail selection step to select eukaryotic mRNA. The libraries were then pooled and sequenced on two lanes of a HiSeqX 150 base pair paired-end platform at Fulgent Genetics (Temple City, CA).

Bioinformatic analyses, library normalization, and transcript CPM calculation

The metatranscriptomic sequence data were analysed using a bioinformatic pipeline that was adapted from a pipeline developed by Hu et al. (2018). Briefly, paired-end metatranscriptomic sequences were trimmed and quality filtered using Trimmomatic v. 0.38 (Bolger et al., 2014). The ERCC spike-in sequences were then aligned to the trimmed reads using Trinity v. 2.8.4 (Grabherr et al., 2011) to confirm that an anticipated number of reads from each sample came from the ERCC spike-in (≈1% of the total reads per sample; Table S2). After counting and removing ERCC reads, the reads from samples that were sequenced on multiple lanes were concatenated and rRNA reads were separated from the read pool by aligning the trimmed reads to the PR2 database v. 12 (Guillou et al., 2013) using SortMeRNA v. 2.1 (Kopylova et al., 2012; Table S3). The sequences that aligned to the PR2 18S rRNA gene database were then annotated at a 97% similarity threshold against the PR2 database using qiime1 (Caporaso et al., 2010). These annotated rRNA sequences were used to evaluate the taxonomic composition of the protistan communities at the eddy sites and depths in downstream analyses. The reads that did not align to the PR2 database were used to assemble metatranscriptomes with the MEGAHIT v. 1.2.8 assembly program (Li et al., 2015). Metatranscriptome co-assemblies were carried out for each site and depth, resulting in eight total assemblies. Following metatranscriptome assembly, the contigs from all assemblies were clustered at a 95% coverage and 97% similarity threshold using MMSeqs2 (Steinegger & Söding, 2018) to eliminate redundant contigs resulting from the eight co-assemblies. Representative contigs were then obtained for each cluster and the transcripts were aligned to these representative contigs using Salmon v. 1.5.1 (Patro et al., 2017). Putative protein-coding sequences were predicted from the representative contigs using GeneMarkS-T v. 5.1 (Tang et al., 2015) and these protein-coding sequences were assigned a taxonomic annotation using EUKulele v. 2.0.3 (Krinos et al., 2021). Kyoto Encyclopedia of Genes and Genomes (KEGG) functional annotations were then assigned to each putative protein-coding sequence where possible, using eggNOG-mapper v. 2.0.1b (Huerta-Cepas et al., 2017, 2019).

Contigs annotated as domain Eukaryota were retained for further analysis. After compiling the taxonomic and functional annotation information associated with each putative protein-coding sequence, the library sizes (corresponding to each eddy-depth pairing) were normalized using the trimmed mean of M-values normalization method (TMM) in edgeR (Lund et al., 2012; R Core Team, 2022; Robinson et al., 2010). These normalized library sizes were used to calculate the counts per million (CPM) for each putative, eukaryotic protein-coding sequence in edgeR (Lund et al., 2012; R Core Team, 2022; Robinson et al., 2010). The library normalization and CPM calculation steps were performed on all putative protein-coding sequences that were annotated as domain 'Eukaryota', and on subsetted datasets that included only putative protein-coding sequences that were annotated as a specific taxonomic group (i.e., chlorophytes, ciliates, diatoms, dinoflagellates, haptophytes, and rhizarians).

Relative expression profiles of phototrophy and heterotrophy biomarker genes

Putative phototrophy and heterotrophy biomarker genes were compiled from the KEGG database and from previous studies to identify potential shifts in protistan community metabolism between the eddy sites. The genes used in this analysis were categorized into various biomarker gene groups based on the specific pathway or process in which each gene is thought to be involved (Table S4). The relative abundances of the transcripts in each of these gene groups were summed for each sample. Then, the sums were standardized by calculating *Z*-scores to visualize shifts in the relative expression of these gene groups across samples. The *Z*-scores for each sample were averaged across triplicates and the standard errors associated with each average were calculated.

The average ratio of all phototrophy-associated transcripts relative to all heterotrophy-associated

transcripts (Table S4) was also calculated for the whole eukaryotic community and six major taxonomic groups (i.e., chlorophytes, dinoflagellates, rhizarians, haptophytes, ciliates, and diatoms). These phototrophy to heterotrophy (phototrophy:heterotrophy) transcript ratios were used to evaluate the potential importance of phototrophic and heterotrophic nutrition between the eddy sites at each of the four sampling depths. To calculate the ratios, the relative abundances of all phototrophy- and heterotrophy-associated transcripts were summed for each replicate sample. Then, the total number of phototrophy-associated transcripts per sample was divided by the total number of heterotrophy-associated transcripts per sample to calculate a ratio. Finally, the ratios associated with samples collected at the same eddy site and depth were averaged and the standard error of each average value was calculated.

Statistical analyses

Two-way analysis of variance (ANOVA) tests were used to determine if depth, eddy polarity, and depth × eddy polarity altered the *Z*-scores calculated for each of the phototrophy- and heterotrophy-associated transcript groups for the whole eukaryotic community. The *p*-values resulting from all of the two-way ANOVAs were then adjusted using a false discovery rate (FDR) correction. Following these two-way ANOVAs, pairwise *t*-tests with pooled standard deviations were used to determine if the mean *Z*-scores of the phototrophy and heterotrophy biomarker transcripts were significantly different between all eddy site and depth combinations. The *p*-values resulting from these pairwise *t*-tests were also adjusted using an FDR correction. The same statistical analysis procedures were used to evaluate the influences of eddy polarity and depth on the phototrophy:heterotrophy transcript ratios for the whole eukaryotic community and for the six major taxonomic groups analysed. Two-way ANOVAs were carried out to assess the effects of eddy polarity, depth, and eddy polarity × depth on these transcript ratios. Then, pairwise *t*-tests with pooled standard deviations were used to determine if the mean phototrophy:heterotrophy transcript ratios were significantly different between each eddy site and depth combination for each taxonomic group. The *p*-values resulting from the ANOVAs and the pairwise *t*-tests were adjusted using an FDR correction.

Dinoflagellate orthologous group identification, differential expression analyses, and KEGG module enrichment

Because many dinoflagellates have particularly flexible nutritional strategies (Cohen et al., 2021; Jeong et al., 2010) and dinoflagellate transcripts comprised a large fraction of the transcript pool, a more in-depth gene expression analysis was performed for this group. The dinoflagellate-specific analysis used orthologous grouping, differential expression analyses, and module enrichment analyses to determine which KEGG modules were differentially expressed between the cyclonic and anticyclonic eddy sites at each sampling depth. GeneMarkS-T v. 5.1 (Tang et al., 2015) was used to identify putative protein-coding sequences for all contigs from the eight metatranscriptomic co-assemblies. These putative protein-coding sequences were then assigned a taxonomic annotation using EUKulele (Krinos et al., 2021) and a custom database that included more dinoflagellate reference sequences from the PhyloDB database (Allen, 2015) as well as bacterial and archaeal reference sequences from MarRef (Klemetsen et al., 2018). Protein sequences that were predicted from the dinoflagellate-specific contigs were then used to create dinoflagellate orthologous groups using OrthoFinder (Emms & Kelly, 2019). KEGG functional annotations were then assigned to the dinoflagellate orthologous groups using eggNOG-mapper (Huerta-Cepas et al., 2017, 2019).

Differential expression analysis was used to identify specific dinoflagellate orthologous groups that were significantly differentially expressed between the eddies at each of the four sampling depths. The differential expression analyses were carried out by normalizing the library sizes for each eddy-depth pairing using the TMM method (Lund et al., 2012; R Core Team, 2022). Then, pairwise differential expression calculations were carried out using the edgeR genewise negative binomial generalized linear model with quasi-likelihood tests ('glmQLFTest' function; Lund et al., 2012; R Core Team, 2022; Robinson et al., 2010). The *p*-values that were associated with each differentially expressed orthologous group were adjusted using an FDR correction. An adjusted *p*-value of 0.01 was used as a cutoff to identify orthologous groups that were significantly differentially expressed between the cyclonic and anticyclonic eddy sites at each depth. The KEGG KO terms that were associated with the significantly ($p_{adj} < 0.01$) differentially expressed orthologous groups in the cyclone and anticyclone at each depth were then used to carry out a KEGG module enrichment analysis using the 'enrichMKEGG' function in the clusterProfiler package in R (Wu et al., 2021). The 'enrichMKEGG' function uses an over-representation analysis algorithm (Boyle et al., 2004) to identify specific KEGG modules that are enriched in a list of KO terms relative to a background list. In the dinoflagellate orthologous group module enrichment analysis, all of the KEGG KO terms that were detected in the dinoflagellate orthologous groups at a given depth were used in the background gene list (Wijesooriya et al., 2022). KEGG modules were considered to be significantly enriched in an eddy at a given depth when the FDR-corrected *p*-value output of the clusterProfiler analysis was <0.05 for a given module. The number of hits to each significantly

enriched module was recorded and used for downstream visualization purposes. In total, two KEGG module enrichment analyses were performed at each of the four sampling depths (i.e., KO terms associated with orthologous groups that were upregulated in the cyclone relative to the anticyclone at each depth and KO terms associated with orthologous groups that were upregulated in the anticyclone relative to the cyclone at each depth).

RESULTS

Environmental setting

The cyclonic eddy was weakening (i.e., corrected SLA was increasing at the eddy centre), and the anticyclonic eddy was stable (i.e., corrected SLA remained at ≈21 cm at the eddy centre) at the time of metatranscriptome sample collection (Figure S1a–e). While a weakening cyclone and a stable anticyclone were apparent when looking at the corrected SLA values observed at the eddy centres over time (Figure S1a–e), those temporal trends in eddy strength were not apparent when looking at the corrected SLAs of the specific cyclonic and anticyclonic eddy sites that were sampled in this study (Figure S1f). The corrected SLAs at both the cyclonic and anticyclonic eddy sampling site decreased slightly leading up to the metatranscriptomic sampling dates (4 April 2018 and 8 April 2018, in the cyclone and anticyclone, respectively; Figure S1f), demonstrating that the temporal trends in corrected SLA at the eddy sites differed from the temporal trends observed at the eddy centres.

A positive corrected SLA at the anticyclonic eddy site (≈17 cm) and a negative corrected SLA at the cyclonic eddy site (≈−12 cm) were observed at the time of sampling (Figure 1A). The potential density in the cyclone was greater than that in a nearby non-eddy region (SLA ≈ 0) between 95 and 250 m depth, while the potential density in the anticyclone was lower than that at the non-eddy region between 30 and 250 m depth (Figure 1B). The density differences that were evident when comparing the potential density profiles at the eddy sites to the non-eddy region were consistent with a shoaling and depression of isopycnal surfaces in the cyclone and anticyclone respectively (Figure 1B). The DCM at the cyclonic eddy site was shallower (112 m) and the water was denser (24.5 kg m^{-3}) than the DCM at the non-eddy site (125 m and 24.3 kg m^{-3}, respectively) and the anticyclonic eddy site (122 m and 24.2 kg m^{-3}, respectively), and is consistent with the upward vertical displacement of waters that occurred in the cyclone (Figures 1C and S2a). The depth of the DCM at the anticyclonic eddy site was similar to that noted at the non-eddy site (Figure 1C), even though the DCM waters in the anticyclone were slightly less dense than those observed in the non-eddy region (Figure S2). The chlorophyll fluorescence at the depth of the DCM was higher at the cyclonic eddy site than at the non-eddy site and the anticyclonic eddy site, with RFU values of 0.59, 0.32, and 0.39 at the cyclonic, non-eddy, and anticyclonic eddy sites, respectively (Figures 1C and S2a). Seawater temperature was slightly higher at the cyclonic eddy site than at the non-eddy and anticyclonic eddy sites at 25 m (Figure 1D); however, at the three deepest sampling depths (DCM, 150 m, and 250 m), the temperatures measured at the cyclonic eddy site were lower than those measured at the non-eddy site (consistent with an upward displacement of waters). Conversely, the temperatures measured at the anticyclonic eddy site were higher than those measured at the non-eddy site at the three deepest sampling depths (consistent with a downward displacement of waters; Figure 1D). The oxycline at the cyclonic eddy site appeared to be shallower than the oxyclines at the non-eddy and anticyclonic eddy sites, in that substantial decreases in oxygen concentration with depth began at ≈80, ≈140, and ≈140 m at the cyclonic eddy site, non-eddy site, and anticyclonic eddy site, respectively (Figure 1E). Dissolved oxygen concentrations at the 2 eddy sites differed by an average of 3.15 μmol L^{-1} from the surface to 250 m depth, with the largest difference occurring near the 150 m sampling depth (at 143 m; Figure 1E). At that depth, the concentration of oxygen in the anticyclone was 17.24 μmol L^{-1} greater than the concentration of oxygen in the cyclone.

The concentrations of inorganic, oxidized nitrogen ($NO_3^- + NO_2^-$) and phosphate (PO_4^{3-}) were very low (<0.05 μM) from 5 to 75 m depth in both eddies and at the non-eddy site (Figure 1F). Deeper in the water column, beginning at ≈100 m, inorganic nutrient concentrations were substantially higher at the cyclonic eddy site than at the anticyclonic eddy and non-eddy sites (Figure 1F), consistent with an upward flux of deep, nutrient-rich waters. Total organic carbon concentrations were similar at the cyclonic, non-eddy, and anticyclonic eddy sites from the surface down to 75 m; however, from 100 to 175 m depth, the TOC concentrations at the cyclonic eddy site were considerably lower than those at the anticyclonic eddy site. The TOC concentrations measured at the non-eddy site from 125 to 175 m were between those measured at the cyclonic eddy site and the anticyclonic eddy site (Figure 1G).

Metatranscriptome assemblies and predicted protein annotations

Eight eukaryotic metatranscriptome co-assemblies generated ≈20.1 M contigs in total. The N50 values of the co-assemblies ranged from 527 to 553 and the

average number of base pairs per contig ranged from 531 to 549 (Table S5). The ≈20.1 M contigs resulting from the assemblies were clustered to obtain ≈17.6 M representative contigs. Approximately 13.8 M putative protein-coding sequences were predicted from the ≈17.6 M representative contigs, and 57.5% (≈8.0 M) of those putative protein-coding sequences were assigned as eukaryotic. These eukaryotic protein-coding sequences were the focus of the subsequent analyses. Approximately half (45.7%) of the protein-coding sequences with a eukaryotic taxonomic assignment were also assigned a KEGG functional annotation (Table S5).

Influence of depth on protistan community composition and metabolic potential

The taxonomic annotations of all contigs revealed that depth was a dominant factor shaping protistan community composition, as would be expected for this deep, open ocean environment (Figure 2). Dinoflagellate transcripts were relatively abundant across all metatranscriptome samples (23.5%–43.3% of transcripts) and were the most abundant at 250 m depth in both eddies (Figure 2; Table S6). Haptophyte transcripts contributed most to the total transcript pool (4.9%–34.6% of transcripts) at 25 m and decreased with depth in both eddies (Figure 2; Table S6). Pelagophyte transcripts were found at higher relative abundances at the DCM and 150 m compared with all other depths sampled and comprised an average of 23.0% of transcripts across the eddy sites at these depths (Figure 2; Table S6). Chlorophyte transcripts were found at higher relative abundances at the DCM, 150 m, and 250 m than they were at the shallowest (25 m) sampling depth in both eddies (Figure 2; Table S6). Diatoms, rhizarians, ciliates, and cryptophytes comprised relatively small fractions of the total transcript pool in either eddy (<7% across all samples). Diatom transcript relative abundances showed no consistent pattern across the sampling depths. Conversely, ciliate, cryptophyte, and rhizarian transcripts were found at higher relative abundances at 250 m compared with the other sampling depths in both eddies, despite their modest contribution to total transcript abundance (Figure 2; Table S6).

Multivariate analyses of the 18S rRNA gene reads and transcripts also indicated that depth played a key role in influencing protistan community composition and metabolic potential (Figures 3 and S3). The annotated 18S rRNA gene reads that were extracted from the metatranscriptomes before assembly were used to carry out a nonmetric multidimensional scaling (NMDS) analysis with Bray–Curtis dissimilarity to visualize taxonomic differences between the two eddies at the four sampling depths. Additionally, a principal component analysis (PCA) plot was created with the relative abundances of transcripts that were assigned KEGG functional annotations to visualize differences in eukaryotic community transcriptional patterns between the eddy sites and depths (Figures 3 and S3). The samples on the NMDS and PCA plots were separated primarily by sampling depth from the DCM to 250 m along the NMDS1 and PC1 axes (Figure 3), indicating that depth strongly influenced both eukaryotic community composition and transcriptional patterns across the DCM to 250 m depth range. Samples collected at 25 m depth clearly separated from the samples collected at the

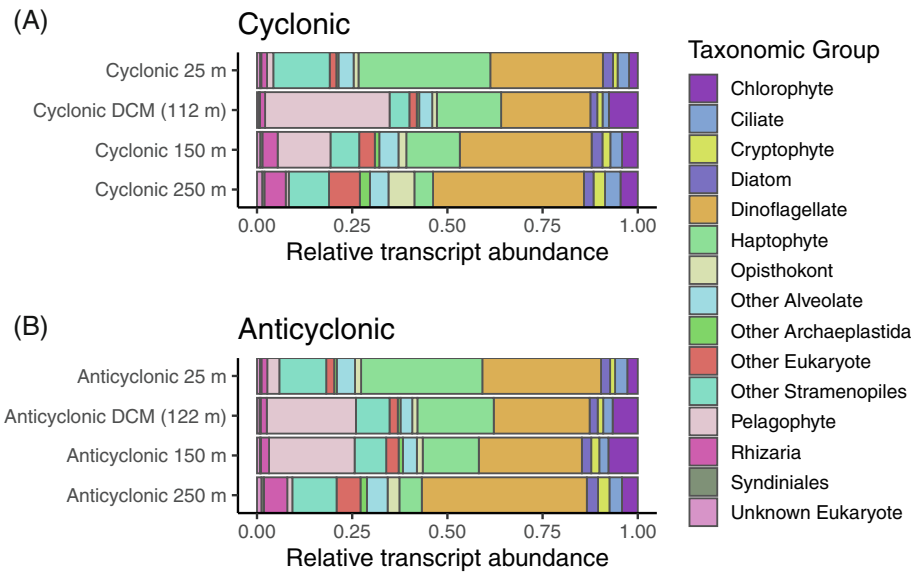

FIGURE 2 Taxonomic breakdown of the transcripts in the cyclonic (A) and anticyclonic (B) eddy samples. The bars depict the average relative abundances of transcripts associated with each taxonomic group across three replicate samples for each eddy and depth combination.

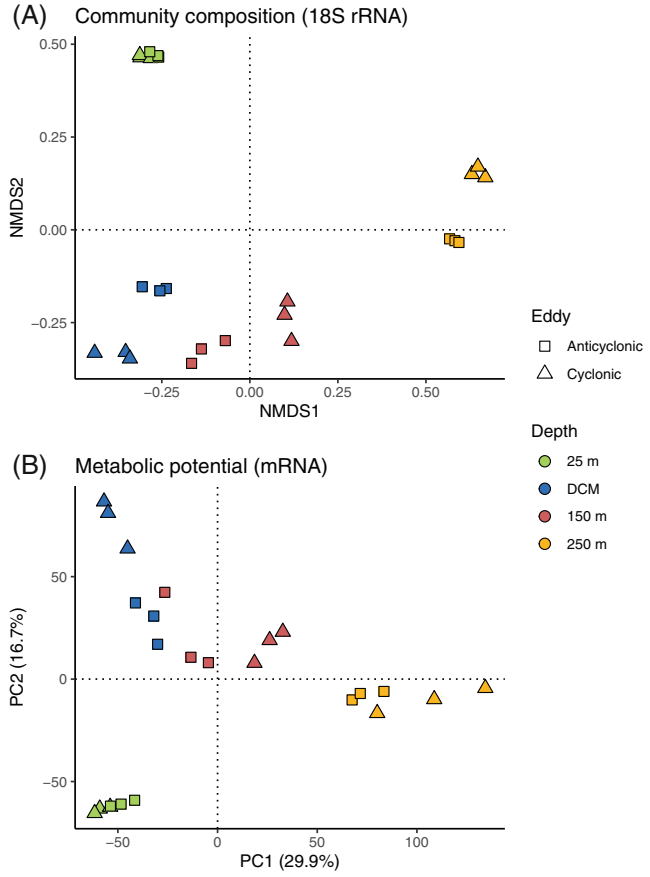

FIGURE 3 Non-metric multidimensional scaling (NMDS; panel A) plot depicting the differences in eukaryotic community composition between the eddy sites and depths as inferred through 18S eukaryotic rRNA sequences. Principal component analysis (PCA; panel B) plot depicting differences in expression of KEGG-annotated, eukaryotic predicted proteins across the eddy sites and sampling depths. Cyclonic eddy sites are represented as triangles, anticyclonic eddy sites are represented as squares, and colours correspond to the sampling depth. Points that are the same shape and colour are replicate samples.

three deeper sampling depths (DCM, 150 m, and 250 m) on the NMDS and PCA plots, suggesting that eukaryotic community composition and metabolic potential noted at the deeper depths differed from those observed at 25 m (Figure 3).

Influence of eddy polarity on protistan community composition and metabolic potential

The notable effects of eddy polarity on protistan community composition and metabolic potential were evident when comparing cyclonic and anticyclonic eddy samples collected at the same depth. In general, the differences in eukaryotic community composition and metabolism between the eddies at 25 m were less pronounced than the differences between the eddies that were evident at the deeper sampling depths (Figure 3; green triangles and squares cluster close to one another while blue, red, and yellow triangles do not cluster with similarly coloured squares). Differences in protistan community metabolic potential between the cyclonic and anticyclonic eddies were most pronounced when using separate, depth-specific PCA plots to visualize differences in community transcriptional patterns between the two eddies (Figure S4). At all four sampling depths and across all replicates, the cyclonic and anticyclonic eddy samples separated from one another along the PC1 axis (Figure S4), indicating that eddy polarity explained a large fraction of the variability in transcriptional patterns between samples that were collected at the same depth in the two locations.

Mesoscale physical features impacted how taxonomically and metabolically similar protistan communities at 150 m were to euphotic (i.e., 25 m and the DCM) and mesopelagic (i.e., 250 m) zone communities. The NMDS and PCA plots revealed that the anticyclonic eddy samples collected at 150 m depth were on average taxonomically and metabolically more similar to the DCM samples than were the samples collected at 150 m depth in the cyclonic eddy (Figure 3; red squares fall on the negative side of the NMDS1 and PC1 axes with the blue shapes). The cyclonic eddy samples collected at 150 m depth did not cluster closely with samples collected at any other depth along the NMDS1 or PC1 axes. However, the cyclonic eddy samples collected at 150 m depth fell on the same side of the NMDS1 and PC1 axes as the mesopelagic samples, indicating that the protistan communities at 150 m in the cyclone were taxonomically and metabolically more similar to the mesopelagic samples than were the anticyclonic eddy communities collected at 150 m depth (Figure 3; red triangles fall on the positive side of the NMDS1 and PC1 axes with the yellow shapes).

Differences in the cyclonic and anticyclonic eddy communities at 150 m depth were further highlighted when the broad taxonomic breakdown of the eukaryotic transcripts at the DCM, 150 m, and 250 m were examined. The average relative abundances of chlorophyte, ciliate, and rhizarian transcripts at 150 m in the anticyclone were more similar to the average relative abundances of these taxonomic groups at the DCM in both eddies than they were to the average relative abundances of these taxonomic groups at 250 m in both eddies (Figure 2; Table S6). The opposite trend was true in the cyclone, in that the average relative abundances of chlorophyte, ciliate, and rhizarian transcripts at 150 m in the cyclone were more similar to the average relative abundances of these taxonomic groups at 250 m in both eddies compared with the average relative abundances of these taxonomic groups at the DCM in both eddies (Figure 2; Table S6).

Effects of depth and eddy polarity on the abundances of phototrophy- and heterotrophy-associated transcripts

Transcripts that were considered phototrophy- or heterotrophy-associated in this study comprised ≈6.9% of the total eukaryotic transcript pool and ≈10.9% of the functionally annotated eukaryotic transcript pool. Depth had a significant effect on the relative abundances of transcripts associated with all of the phototrophy and heterotrophy biomarker gene groups examined in this study ($p_{adj} < 0.01$ for all gene groups, two-way ANOVA; Figure 4; Table S7). The relative abundances of photosynthesis, Calvin cycle, and inorganic nitrogen metabolism transcripts were generally higher at 25 m and the DCM, but lower at the deeper sampling depths in both eddies (Figure 4A–C). The relative abundance patterns of transcripts associated with antenna proteins differed from the relative abundance patterns of the photosynthesis, Calvin cycle, and inorganic nitrogen metabolism transcript groups in that the relative abundances of transcripts associated with antenna proteins peaked at the intermediate depths (i.e., DCM and 150 m) as opposed to 25 m and the DCM (Figure 4D). There were no consistent trends in the relative abundances of the heterotrophy-associated transcripts with depth. The relative abundances of transcripts associated with some of the heterotrophy biomarker gene groups were highest in euphotic zone samples (i.e., phagosome, V-type ATPase, fatty acid breakdown; Figure 4E–G), while the relative abundances of transcripts associated with other heterotrophy biomarker gene groups were highest at 250 m (i.e., cathepsin, Rho GTPase; Figure 4H,I).

There were some differences between the eddies in the relative abundances of transcripts associated with the phototrophy and heterotrophy biomarker gene groups. The average relative abundances of photosynthesis-related transcripts, Calvin cycle-related transcripts, and inorganic nitrogen metabolism-related transcripts were significantly different in the anticyclone and cyclone at the depth of the DCM ($p_{adj} < 0.05$, pairwise *t*-test; Table S7) with the average relative abundances of the photosynthesis- and Calvin cycle-related transcripts being higher in the cyclone relative to the anticyclone, and the average relative abundance of the inorganic nitrogen metabolism transcripts being higher in the anticyclone relative to the cyclone (Figure 4A–C). Photosynthesis-related transcripts and antenna protein-related transcripts were significantly different between the cyclonic and anticyclonic eddy sites at 150 m ($p_{adj} < 0.01$, pairwise *t*-test; Table S7), and the average abundances of these transcript groups were higher in the anticyclone relative to the cyclone at this depth (Figure 4A,D).

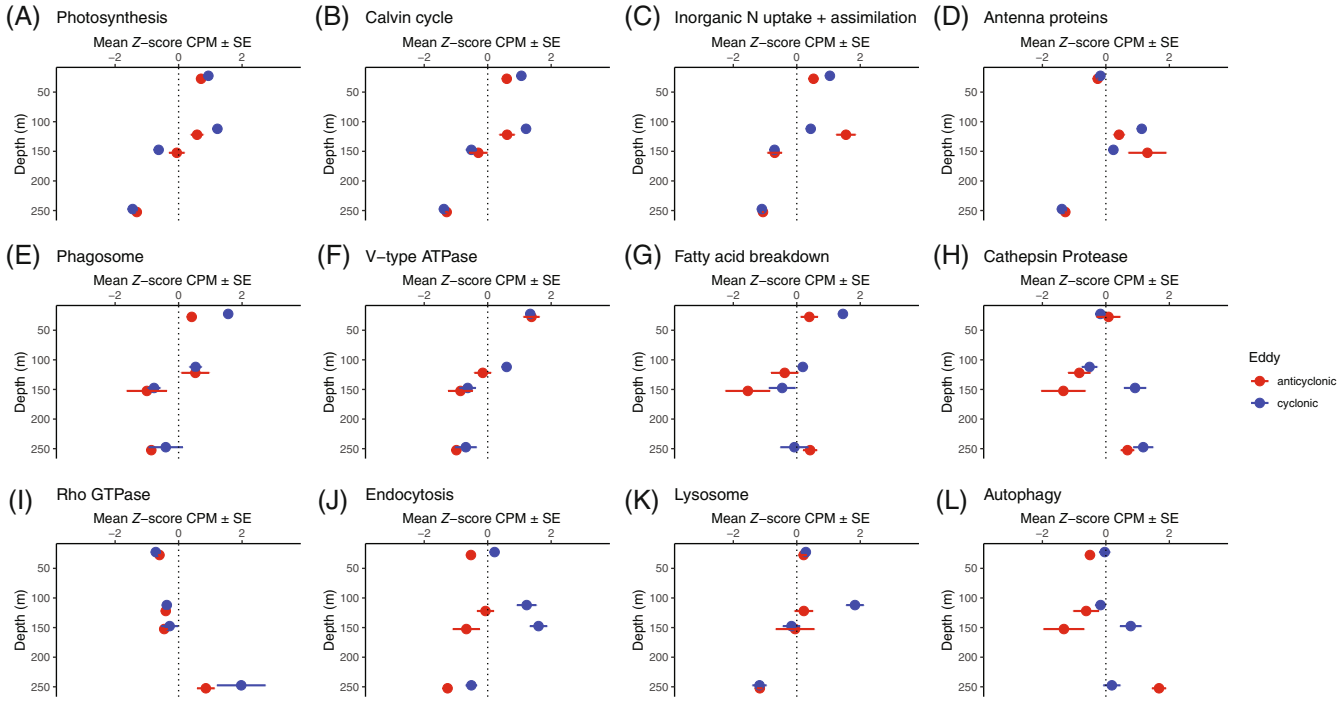

FIGURE 4 Relative expression (*Z*-score standardized expression) of various phototrophy and heterotrophy biomarker gene groups at the two eddy sites and four sampling depths for all eukaryotic taxa. Photosynthesis, Calvin cycle, and antenna protein (A,B,D) gene groups were considered phototrophy biomarkers, while phagosome, V-type ATPase, fatty acid breakdown, cathepsin protease, Rho GTPase, endocytosis, lysosome, and autophagy (E–L) gene groups were considered heterotrophy biomarkers. KEGG KO terms associated with each gene group are listed in Table S4. Each point represents the average Z-score standardized transcript abundance across three replicate samples for each eddy site and depth. Error bars show ± SE associated with each average value.

Heterotrophy-associated transcripts were generally found at higher average relative abundances in the cyclonic eddy samples than in the anticyclonic eddy samples when the average relative abundances of heterotrophy-associated transcripts were significantly different between the eddy sites at a given depth. For example, the relative abundances of endocytosis- and lysosome-associated transcripts were significantly different at the DCM of the cyclonic eddy relative to the DCM of the anticyclonic eddy ($p_{adj} < 0.01$, pairwise *t*-test; Table S7) with the DCM of the cyclonic eddy having higher average relative abundances of these transcripts (Figure 4J,K). The average relative abundances of cathepsin protease, endocytosis, and autophagy transcripts were significantly different at the eddy sites at 150 m depth ($p_{adj} < 0.01$, pairwise *t*-test; Table S7) and these transcripts were found at higher average relative abundances at the cyclonic eddy site relative to the anticyclonic eddy site at this depth (Figure 4H,J,L).

The observed effects of depth and eddy polarity on the relative abundances of the phototrophy- and heterotrophy-associated transcripts differed for major taxonomic groups and the biomarker gene groups (Figure S5). The average ratio of all phototrophy-associated transcripts relative to all heterotrophy-associated transcripts (phototrophy:heterotrophy ratio; Table S4) was calculated for the whole microbial eukaryote community (Figure 5A) and for six different protistan taxa at each of the eddy sites and sampling depths (Figure 5B–G) to simplify the differences across groups. The average phototrophy:heterotrophy transcript ratio was highest in the 25 m samples for chlorophytes and dinoflagellates (Figure 5B,C). For some of the other taxonomic groups analysed, such as the rhizarians and haptophytes, the highest average phototrophy:heterotrophy transcript ratios were observed at intermediate depths (DCM or 150 m; Figure 5D,E). These high, taxon-specific phototrophy:heterotrophy transcript ratios observed at the DCM and 150 m were often observed in only one of the eddies at a given depth, highlighting the important role that eddy polarity may play in influencing the nutritional physiology of specific protistan groups at those depths. For example, the average phototrophy:heterotrophy transcript ratios were significantly different between the eddy sites at the depth of the DCM for chlorophytes and rhizarians ($p_{adj} < 0.05$, pairwise *t*-test; Table S8), and these ratios were higher in the anticyclonic eddy DCM than in the cyclonic eddy DCM (Figure 5B,D). The average phototrophy:heterotrophy transcript ratios were also significantly different between the eddy sites at the depth of the DCM for dinoflagellates and haptophytes ($p_{adj} < 0.01$, pairwise *t*-test; Table S8), with the ratios in the cyclone being higher than those in the anticyclone for these taxonomic groups (Figure 5C,E). There were significant differences in the mean phototrophy:heterotrophy transcript ratios observed in the two eddies at 150 m depth for all of the taxonomic groups analysed except ciliates ($p_{adj} < 0.05$, pairwise *t*-test; Table S8). At this depth, the average phototrophy:heterotrophy transcript ratios were higher in the anticyclonic eddy relative to the cyclonic eddy for all eukaryotes, chlorophytes, dinoflagellates, rhizarians, haptophytes, and diatoms (Figure 5A–E,G), suggesting that eddy polarity had a pronounced influence on the nutritional physiology of protists at 150 m depth. These differences

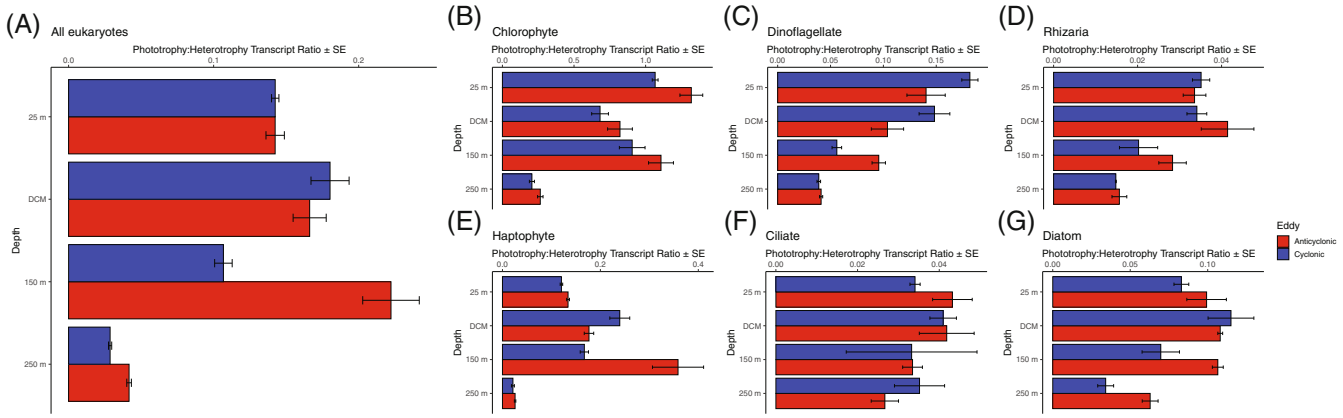

FIGURE 5 Average phototrophy to heterotrophy (phototrophy:heterotrophy) transcript ratios for all eukaryotes (A) and for major protistan taxonomic groups (B–G) in the cyclonic and anticyclonic eddies at the four sampling depths. The phototrophy:heterotrophy transcript ratios denote the potential importance of phototrophic nutrition compared with heterotrophic nutrition between the eddy sites at each of the four sampling depths. Relative transcript abundances were calculated for each taxonomic group before calculating the transcript ratios (using TMM library normalization and CPM calculation procedures in edgeR; see Section 2). Photosynthesis, Calvin cycle, and antenna protein gene groups were considered phototrophy biomarkers, while phagosome, V-type ATPase, fatty acid breakdown, cathepsin protease, Rho GTPase, endocytosis, lysosome, and autophagy gene groups were considered heterotrophy biomarkers. The KEGG KO annotations for the phototrophy- and heterotrophy-associated transcripts are listed in Table S4. Each bar represents the average transcript ratio across three replicate samples for each eddy site and depth. Error bars show ± SE associated with each average value.

in the phototrophy:heterotrophy transcript ratios observed at 150 m depth were further highlighted when noting the higher *Z*-score standardized abundances of autophagy, cathepsin protease, endocytosis, and lysosome-associated heterotrophy biomarker genes at 150 m in the cyclone relative to the anticyclone for dinoflagellates and rhizarians (Figure S5d,f). Conversely, the *Z*-score standardized abundances of photosynthesis-related genes at 150 m were higher in the anticyclone relative to the cyclone for primarily phototrophic groups such as the chlorophytes and diatoms (Figure S5a,c). The lowest average phototrophy:heterotrophy transcript ratios were generally observed at 250 m for all of the taxa analysed (Figure 5), as anticipated.

Differential expression and KEGG module enrichment of dinoflagellate orthologous groups

Dinoflagellate transcripts were abundant in the metatranscriptomes collected in this study (Figure 2, Table S6), making it possible to identify metabolic differences in the cyclonic and anticyclonic eddy dinoflagellates. Thousands of dinoflagellate orthologous groups were significantly differentially expressed ($p_{adj} < 0.01$) between the eddy sites at all depths; however, only 8, 8, and 14 KEGG modules were significantly ($p_{adj} < 0.05$) enriched at 25 m, the DCM, and 150 m, respectively (Figures 6 and S6). No KEGG modules were significantly enriched at the 250 m sampling depth.

The module enrichment analysis of the differentially expressed orthologous groups revealed that all of the significantly ($p_{adj} < 0.05$) enriched modules at the DCM were enriched in the cyclone relative to the anticyclone, while the majority of the significantly enriched modules at 150 m were enriched in the anticyclone relative to the cyclone (Figure 6). Many of the modules that were enriched in the DCM of the cyclonic eddy relative to the DCM of the anticyclonic eddy were involved in carbon metabolism (i.e., glycolysis, gluconeogenesis, and Calvin cycle), amino acid biosynthesis (i.e., tryptophan biosynthesis), and cellular respiration (i.e., citrate cycle; Figure 6A). At 150 m depth, modules associated with

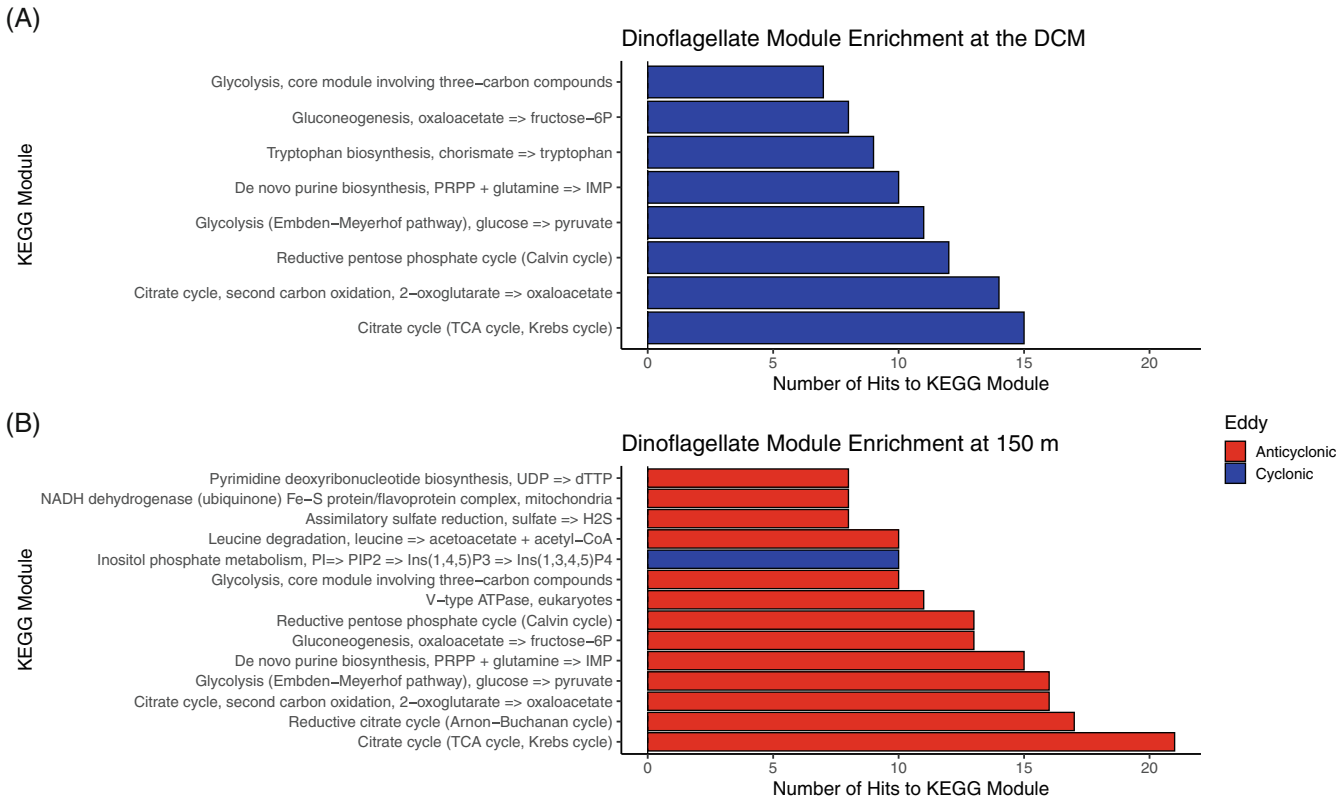

FIGURE 6 KEGG modules that were significantly ($p_{adj} < 0.05$) enriched in the differentially expressed dinoflagellate orthologous groups at the DCM (A) and 150 m depth (B). Dinoflagellate orthologous groups that were significantly ($p_{adj} < 0.01$) differentially expressed between the eddy sites at each depth were compiled and the KEGG KO terms assigned to these differentially expressed orthologous groups were used as input in the enrichment analyses. Blue bars denote modules that were significantly enriched in the cyclone relative to the anticyclone at each depth, while red bars denote modules that were significantly enriched in the anticyclone relative to the cyclone at each depth. Module enrichment analyses for the cyclonic and anticyclonic eddies were carried out separately at each depth. The *x*-axes show the number of KEGG KO terms that were associated with a given module in the enrichment analysis. The differential expression analyses were carried out using the edgeR package in R, while the module enrichment analyses were carried out using the clusterProfiler package in R (see Section 2).

carbon metabolism (i.e., glycolysis, gluconeogenesis, and Calvin cycle), amino acid degradation (i.e., leucine degradation), and cellular respiration (i.e., citrate cycle) were enriched in the anticyclone relative to the cyclone. Only one module was enriched in the cyclone relative to the anticyclone at 150 m and was associated with inositol phosphate metabolism (i.e., cell signalling processes; Figure 6B).

Many of the KEGG modules that were enriched in the DCM of the cyclone were enriched at 150 m depth in the anticyclone. For example, modules associated with carbon metabolism (i.e., glycolysis gluconeogenesis, and Calvin cycle) were significantly enriched in the anticyclone at 150 m depth, and these same modules were enriched in the cyclone at the DCM (Figure 6). Similarly, modules associated with the citrate cycle and purine biosynthesis were enriched in the anticyclonic eddy at 150 m depth and in the cyclonic eddy at the DCM (Figure 6). At the DCM and 150 m depth, the citrate cycle modules were some of the most enriched in the cyclone and anticyclone respectively (Figure 6).

DISCUSSION

Identifying how mesoscale physical forcing impacts protistan community composition and function is critical to understanding the potential importance of eddies in affecting the production and export of organic carbon in the ocean. The overall goal of this study was to determine how protistan community composition and transcriptional patterns responded to mesoscale eddies of opposite polarity and whether the effects of these eddies on protistan communities varied with depth. Eukaryotic metatranscriptomes obtained at various depths in the water column in a cyclonic and an anticyclonic mesoscale eddy were first used to identify how eddies impacted the composition and metabolism of the protistan community. Changes in the expression of genes that may be associated with phototrophic and heterotrophic processes were then examined to determine if shifts in the physiochemical environment resulting from the contrasting physical forcing of the eddies altered the nutritional physiology of euphotic and mesopelagic protists in the NPSG.

Mesoscale eddies altered the biogeochemical properties of NPSG waters

The eddies that were sampled in this study were generally characteristic of cyclonic and anticyclonic eddy systems that have been previously studied in the NPSG. The relatively high potential density of waters below 95 m depth in the cyclone was consistent with a shoaling of isopycnal surfaces and led to a shallower DCM depth at the cyclonic eddy site (Barone et al., 2022; Cornec et al., 2021; Xiu & Chai, 2020; Figure 1B,C). The higher chlorophyll fluorescence observed at the DCM of the cyclonic eddy site relative to that of the non-eddy site has been explained by higher abundances of eukaryotic phytoplankton but lower abundances of picocyanobacteria at the DCM of cyclones (Barone et al., 2019, 2022; Vaillancourt et al., 2003; Figure S7). The higher chlorophyll fluorescence observed at the DCM of the anticyclonic eddy site relative to that of the non-eddy site in the present study (Figure 1C) may be due to higher N_2 fixation rates occurring in the anticyclone. Previous studies have revealed that anticyclonic eddy systems have the potential to promote N_2 fixation in the NPSG, which may ultimately enhance phytoplankton biomass accumulation in euphotic waters due to increases in bioavailable nitrogen (Church et al., 2009; Dugenne et al., 2023; Fong et al., 2008).

The higher inorganic nutrient concentrations and lower oxygen concentrations below the DCM at the cyclonic eddy site relative to the non-eddy and anticyclonic eddy sites (Figure 1E,F) were also expected based on previous studies that have linked these differences to the vertical displacement of phytoplankton communities in eddy centres (Barone et al., 2019, 2022; Xiu & Chai, 2020). A shallower DCM in the cyclonic eddy increased light availability to a community that would otherwise be strongly light-limited, ultimately supporting more primary productivity and leaving behind the physiochemical signatures of previous increases in production above the DCM depth (i.e., relatively high oxygen concentrations and low inorganic nutrient concentrations; Barone et al., 2022; Cornec et al., 2021; McGillicuddy, 2016; Figure 1E,F). Below the DCM depth, oxygen concentrations in the cyclonic eddy were relatively low, and inorganic nutrient concentrations were relatively high (Figure 1E,F), consistent with the expectation of increased organic matter remineralization below the DCM in cyclonic eddies (Buesseler et al., 2008; McGillicuddy et al., 2007; Sukigara et al., 2014; Figure 1E,F).

The life phases of the eddies sampled in this study must be considered in the interpretation of our metatranscriptome results, as eddy biogeochemistry has been shown to change throughout eddy lifespans (Barone et al., 2022; Huang et al., 2017; Siegel et al., 2008). The cyclonic eddy sampled in this study was weakening at the time of metatranscriptome sample collection (Figure S1), which likely influenced the composition and metabolism of the protistan communities that were observed in these waters. For example, previous studies that have characterized phytoplankton communities in cyclonic eddies in the NPSG have reported high relative abundances of diatoms at relatively shallow DCM depths (60–80 m depth; Benitez-Nelson et al., 2007; Brown et al., 2008; Letelier et al., 2000). High relative abundances of diatoms at the cyclonic eddy DCM were not apparent in the current

study (Figure 2A, Table S6), presumably due to the weakening state of the eddy. The cyclonic eddy samples collected in the current study were likely representative of the post-intensification state of cyclonic eddies described by Barone et al. (2022). During this post-intensification phase, the previously uplifted DCM inside of a cyclonic eddy begins to deepen again, and the nutrient requirements of the phytoplankton in the DCM are sustained through turbulent mixing across the pycnocline (Barone et al., 2022).

The distance between the cyclonic and anticyclonic eddy sites sampled in this study and the true eddy centres (i.e., site where the corrected SLA was the highest in the anticyclone and lowest in the cyclone) must also be considered in the interpretation of our transcriptional results, as previous studies have reported spatial variability in eddy biogeochemistry (e.g., Brown et al., 2008; Cotti-Rausch et al., 2016). For example, a study that characterized an NPSG cyclonic eddy revealed that chlorophyll *a* concentrations and phytoplankton biomass estimates at the DCM of the eddy generally decreased with distance from the eddy centre (Brown et al., 2008). Additionally, other physical dynamics such as interactions between mesoscale eddies and the ambient chlorophyll field (McGillicuddy, 2016), interactions between two eddies (Guidi et al., 2012), or interactions between eddies and wind stress (McGillicuddy, 2016; Siegel et al., 2008) could differentially impact the biogeochemical properties of waters within a given eddy. Future studies that characterize microbial community composition and metabolism across cyclonic and anticyclonic eddies (i.e., from eddy centres to eddy edges) will be needed to characterize how variable the transcriptional signals identified in the current study are across eddy dipoles.

Depth played a major role in shaping eukaryotic community composition and transcriptional patterns across the entire depth range sampled

The composition and metabolic potential of the protistan communities sampled in this study were strongly influenced by depth at both eddy sites (Figures 2 and 3). Such a finding is consistent with the expectation of the dramatic effect of depth on the chemical/physical environmental conditions (and thus on the biota) in this deep ocean ecosystem. Changes in the taxonomic composition of the transcript pool with depth were generally similar at the cyclonic and anticyclonic eddy sites (Figure 2) and were consistent with previous studies that have documented depth-related shifts in the metabolically active members of oceanic protistan communities (Giner et al., 2020; Hu et al., 2018; Ollison et al., 2021). A recent metabarcoding study by Ollison et al. (2021) found that the relative abundance of rhizarian 18S rRNA reads generally increased with depth from 5 to 770 m in the NPSG and similar increases in rhizarians with depth were observed in the 18S rRNA and transcript abundance data in the current study (Figure 2, Table S6). Additionally, the Ollison et al. (2021) study and a global ocean metabarcoding study carried out by Giner et al. (2020) revealed that the relative abundances of pelagophyte 18S rRNA reads were higher in DCM and lower euphotic zone (100–175 m) samples relative to surface and mesopelagic samples. The results of the current study agree with those obtained by Ollison et al. (2021) and Giner et al. (2020) in that higher relative abundance of pelagophyte transcripts and 18S rRNA reads were observed at the DCM and 150 m sampling depths relative to the 25 m and 250 m sampling depths in both eddies (Figure 2, Table S6).

Changes in the nutritional physiology of the protistan community with depth were apparent in the transcriptional data obtained in this study. The lower relative abundances of photosynthesis and Calvin cycle transcripts at the deeper depths (i.e., 150 and 250 m) relative to the shallower depths (i.e., 25 m and the DCM; Figure 4A,B) and the relatively low phototrophy:heterotrophy transcript ratios that were observed at 250 m depth in this study (Figure 5) were consistent with decreased primary production as light attenuates with depth (Karl & Church, 2017). Similar decreases in the abundances of phototrophy-associated transcripts with depth were observed in previous metatranscriptome studies that have been carried out in euphotic and mesopelagic waters (Cohen et al., 2021; Hu et al., 2018). The transcriptional data obtained in these studies and in the current study support the notion that protists living at sub-euphotic depths (where light becomes limiting) were less reliant on photosynthetically derived organic carbon and consequently more reliant on ingested organic carbon due to limited light availability in mesopelagic waters.

Eddy polarity had a pronounced influence on protistan communities within a given depth

Differences in protistan community composition and metabolism between the eddy sites in this study were apparent at depths below 25 m when comparing samples collected at the same depth from the cyclonic and anticyclonic eddies (Figure 3). One simple explanation for this finding was the effect that eddy type had on the physiochemical environment in the middle and lower euphotic zone (i.e., >100 m depth). A recent study by Barone et al. (2022) documented notable differences in the concentrations of chlorophyll *a*, oxygen, and inorganic nutrients in the lower euphotic zone of eddies of opposite polarity. Indeed, differences in chlorophyll fluorescence (Figure 1C), dissolved oxygen concentration (Figure 1E), $NO_3^- + NO_2^-$ concentration (Figure 1F),

and PO_4^{3-} concentration (Figure 1F) were evident between the eddies at the DCM and 150 m in the current study and presumably influenced some of the transcriptional patterns that were observed. One example of this effect was the higher relative abundances of inorganic nitrogen metabolism transcripts observed at the DCM in the anticyclonic eddy relative to the cyclonic eddy (Figure 4C). This can be explained by the low $NO_3^- + NO_2^-$ concentrations that were observed in the anticyclone relative to the cyclone at this depth (Figure 1F), as previous studies have demonstrated that phytoplankton increase the expression of genes associated with nitrogen uptake and assimilation during periods of nitrogen starvation (Bender et al., 2014; Berg et al., 2008).

The taxonomic and metabolic differences observed among protistan communities at and below the DCM can be explained when considering the capacity that eddies have to vertically displace water layers (McGillicuddy et al., 1998; Nencioli et al., 2008). For example, the upward water column shift that presumably occurred in the cyclonic eddy centre in this study resulted in deeper waters (and the protistan communities living in those waters) being 'moved up' in the water column. This vertical displacement caused the cyclonic eddy protistan communities at 150 m depth to be taxonomically and metabolically more similar to those observed at 250 m depth than were the protistan communities in the anticyclonic eddy at 150 m depth (Figure 3). The impacts that such eddy-induced water column shifts have on picoeukaryote community composition were previously highlighted in a study carried out by Rii et al. (2022) in the NPSG. Using metabarcoding data, Rii et al. (2022) found that when SLA was negative (i.e., upward displacement of the water column), taxa that were typically found in high relative abundances at 175 m depth (e.g., Polycystinea; a group of rhizarians) were found at higher relative abundances at 150 m depth. The metatranscriptomic data that were analysed in the current study augment the work carried out by Rii et al. (2022) by revealing that the vertical shifts that occurred as a result of mesoscale physical forcing altered both the taxonomic composition and the metabolic potential of the protistan communities at the eddy sites (Figures 3, S3, and S4).

Differences in the composition and quantity of sinking material may also explain, at least in part, the distinct transcriptional patterns that were observed between the eddy sites in this study. Cyclonic eddies have been associated with increases in the flux of particulate silica and particulate inorganic carbon out of the euphotic zone and into deeper waters (Barone et al., 2022; Rii et al., 2008; Zhou et al., 2021). Previous analyses carried out in the NPSG have documented notable differences in the composition of protistan communities associated with various particle export events, suggesting that sinking material can alter the structure and function of these communities (Boeuf et al., 2019; Poff et al., 2021). Therefore, the variability in protistan community composition and metabolic potential that was observed in eddies of opposite polarity at lower euphotic and sub-euphotic depths in this study may relate in part to differences in the quantity and quality of sinking material inside of the eddy centres.

Heterotrophy-associated transcripts were found at higher relative abundances in the cyclone compared to the anticyclone on average

The most pronounced differences in protistan community metabolism between the eddies were evident when comparing the average relative abundances of heterotrophy-associated transcripts in the cyclone and anticyclone at 150 m depth. The higher relative abundances of heterotrophy-associated transcripts (Figure 4H,J,L) along with the lower average phototrophy:heterotrophy transcript ratios that were observed in the cyclone relative to the anticyclone at 150 m (Figure 5A–E,G) imply that the protistan community in the cyclone exhibited a more heterotrophic lifestyle at this depth as a result of cyclone-induced changes in the surrounding environment. The differences in the nutritional physiology of the protistan community in the cyclone and anticyclone at 150 m depth may be partially associated with changes in the feeding behaviours of mixotrophic protists. While low inorganic nutrient availability has been shown to increase the relative importance of heterotrophy in mixotrophic protists (Jeong et al., 2010; Stoecker, 1998), the measured N:P ratio at 150 m was higher in the cyclone relative to the anticyclone in the current study, suggesting that nutrient limitation was not the primary factor driving this shift toward heterotrophy (N:P was ≈10 and ≈3 in the cyclone and anticyclone, respectively). Decreases in light availability have also been shown to increase the relative importance of heterotrophic nutrition in mixotrophic protists (Jeong et al., 2010; Stoecker, 1998) and may have influenced the shift toward heterotrophy that occurred at 150 m depth in the cyclone relative to the anticyclone. It is also possible that cyclone-induced changes in the microbial community at 150 m depth increased the availability of suitable prey species in these waters and contributed to the shift toward a heterotrophic nutritional strategy (Jeong et al., 2004; Jeong et al., 2010). Previous studies in the NPSG have documented increases in microzooplankton biomass (Benitez-Nelson et al., 2007; Bidigare et al., 2003; Brown et al., 2008), and grazing rates (Décima & Landry, 2020; Landry et al., 2008) in cyclonic eddy centres as a result of increased primary production and phytoplankton biomass inside these eddies. Similarly, a study carried out in the Mediterranean Sea found that the primary production rate in a cyclonic eddy centre was much greater than

that in an anticyclonic eddy centre and that mesozooplankton grazing accounted for a much higher fraction of the daily phytoplankton stock in this cyclonic eddy centre relative to the anticyclonic eddy centre (i.e., 224% vs. 38% of the phytoplankton stock; Belkin et al., 2022). The results of these previous studies, in combination with the transcriptional data obtained in the current study, imply that eddies invoke measurable shifts in taxonomic composition and physiological processes that affect phototrophy and heterotrophy within the eukaryotic community at depths near the base of the euphotic zone.

Environmental measurements collected during the cruise also support a shift toward a more heterotrophic protistan community as a result of cyclone-induced changes in the environment. There were notable decreases in the concentrations of oxygen and TOC from 75 to 150 m in the cyclonic eddy (Figure 1E,G), which are consistent with a shift toward a more heterotrophic protistan community. Increases in heterotrophic activity would cause organic carbon to be respired back into inorganic carbon (Calbet & Landry, 2004; Worden et al., 2015) and would therefore result in decreases in the ambient oxygen and TOC concentrations in the cyclone if these respiratory losses were not also balanced by increases in phototrophic metabolism.

The shift toward a more heterotrophic protistan community in the lower euphotic zone of the cyclonic eddy has potentially important consequences in the context of carbon cycling and export processes, given that protistan grazing can directly or indirectly alter the amount of carbon that is exported out of the euphotic zone (Steinberg & Landry, 2017; Worden et al., 2015). An early study carried out by Bidigare et al. (2003) in the NPSG found that cyclone-induced local upwelling led to increases in primary production and organic carbon export out of the euphotic zone. However, efforts following Bidigare et al. (2003) found that cyclone-driven particulate organic carbon (POC) export in the NPSG was not substantial, as a large fraction of the newly synthesized organic carbon was remineralised in the euphotic zone (Benitez-Nelson et al., 2007; Maiti et al., 2008; Rii et al., 2008). Additionally, Barone et al. (2022) found evidence that phytoplankton net production increased inside cyclonic eddies in the NPSG but that these increases in net production were not associated with increases in POC export. The lack of a significant POC export event following cyclone-induced increases in phytoplankton production may be explained in part by increases in protistan heterotrophy, given that protistan herbivory may be a substantial sink of phytoplankton production (Calbet & Landry, 2004; Sherr & Sherr, 1994). Additionally, previous observations made in the NPSG have revealed that cyclonic eddy activity may result in increases in the prevalence and export of empty diatom frustules and particulate silica (Barone et al., 2022; Benitez-Nelson et al., 2007; Brown et al., 2008; Maiti et al., 2008; Zhou et al., 2021). These empty diatom frustules and high particulate silica export events could be explained by protistan grazing behaviours, as many protistan grazers have been shown to consume the organic material inside of diatom cells and leave behind the empty frustules (Jacobson & Anderson, 1986; Suttle et al., 1986) or produce faecal pellets that are primarily composed of particulate silica following diatom ingestion (Buck et al., 2005; Sherr & Sherr, 2007).

We show in this study that transcript relative abundance data provide a promising avenue to identify shifts in the nutritional physiology of protists. However, changes in the relative abundances of phototrophy- and heterotrophy-associated transcripts across samples must be evaluated in the context of known nutritional strategy information for specific taxonomic groups, as many of the enzymes that are involved in phototrophic and heterotrophic nutritional processes are also involved in other pathways (Labarre et al., 2020; Obiol et al., 2023; Rogers & Keeling, 2004; Yutin et al., 2009). For example, endocytosis and V-type ATPases are thought to be involved in the uptake of food contents and the acidification of phagosomes in heterotrophic protists (Hu et al., 2018; Labarre et al., 2020); however, transcripts associated with these processes can also be involved in other pathways that are not related to heterotrophy. Diatoms, which are considered a primarily phototrophic protist group, use an endocytosis-mediated process to take up siderophore-bound iron (Kazamia et al., 2018) and V-type ATPases to maintain an acidic pH inside of silica deposition vesicles (Yee et al., 2019). These aspects of diatom biology may contribute to the relatively low phototrophy:heterotrophy transcript ratios we observed among this primarily photosynthesizing group (Figure 5G). Similarly, some enzyme families that are involved in inorganic carbon fixation, such as glyceraldehyde-3-phosphate dehydrogenase and fructose-bisphosphate aldolase, are also involved in other carbon metabolism pathways that are not directly related to photosynthesis (e.g., glycolysis and gluconeogenesis; Gaston & Roger, 2013; Rogers & Keeling, 2004). Heterotrophic protists can therefore express certain genes that are thought to be phototrophy-related, as was observed in a ciliate transcriptomic study by Santoferrara et al. (2014) and in an environmental context in the present study (Figure 5). Despite present caveats that exist when using transcript relative abundance data to identify shifts in the nutritional physiology of protists, the higher relative abundances of phototrophy-related transcripts at 150 m in the anticyclone relative to the cyclone (Figure 4A,D) and the higher relative abundances of specific heterotrophy-related transcripts in the cyclone relative to the anticyclone (Figure 4H,J,L) were consistent patterns that were observed in the current study and enable us to draw general conclusions about shifts in the nutritional physiology of the protistan communities across the eddy sites.

Eddy-induced vertical displacement of water layers affected the metabolism and nutritional physiology of dinoflagellates at the DCM and 150 m depth

Dinoflagellates at the DCM and 150 m depth exhibited a metabolic response to the vertical displacement of waters that occurred in the eddy centres. This metabolic response was evident when considering that a large majority of the carbohydrate metabolism and energy metabolism modules (e.g., glycolysis, citrate cycle, Calvin cycle) that were significantly enriched at the DCM sampling depth were enriched in the cyclone relative to the anticyclone, while the opposite trend was true at the 150 m sampling depth (Figure 6). The enrichment of these carbohydrate and energy metabolism modules at shallower depths in the cyclone relative to the anticyclone is consistent with the upward and downward displacement of waters that presumably occurred in the cyclonic and anticyclonic eddy centres, respectively. These shifts in dinoflagellate metabolism that were noted between the eddies at the DCM and 150 m sampling depths were not associated with notable differences in dinoflagellate taxonomic composition (Figure S8d), suggesting that differences in the expression of specific orthologous groups at these depths resulted from metabolic adjustments as opposed to compositional changes in the dinoflagellate community.

Some of the dinoflagellate metabolic shifts that were noted between the eddies at the DCM and 150 m sampling depths were presumably related to changes in the nutritional physiology of mixotrophic dinoflagellates, given that many dinoflagellates are mixotrophic (Hansen, 2011; Jeong et al., 2010) and a mixotrophic nutritional strategy may provide these organisms with a competitive advantage in nutrient-limited environments like the NPSG (Cohen et al., 2021; Ward, 2019). The enrichment of a Calvin cycle module at the DCM and 150 m in the cyclonic and anticyclonic eddies, respectively, revealed that phototrophy was an important source of organic carbon for dinoflagellates at these eddy sites and depths (Figure 6). The increased importance of phototrophic metabolism in the cyclone relative to the anticyclone at the depth of the DCM and in the anticyclone relative to the cyclone at 150 m depth for dinoflagellates was further supported when evaluating the phototrophy:heterotrophy transcript ratios at the DCM and 150 m sampling depths (Figure 5C). Enrichment of the glycolysis module at the DCM of the cyclone and at 150 m in the anticyclone may also be related to increases in the importance of phototrophic nutrition, given that the expression of specific genes that are involved in glycolysis may increase when dinoflagellates utilize a phototrophic nutritional strategy. A proteomic study of the mixotrophic dinoflagellate, *Prorocentrum micans*, revealed that glyceraldehyde-3-phosphate dehydrogenase (an enzyme involved in glycolysis, gluconeogenesis, and the Calvin cycle) was only expressed when *P. micans* was growing autotrophically (Shim et al., 2011). Another study carried out by Cohen et al. (2021) revealed that dinoflagellate transcript and protein abundances for two enzymes found in the glycolysis, gluconeogenesis, and Calvin cycle pathways (i.e., fructose-bisphosphate aldolase and glyceraldehyde-3-phosphate dehydrogenase) were found at higher abundances in the euphotic zone relative to the mesopelagic zone, along with enzymes involved in photosynthesis and carbon fixation processes (e.g., ferredoxin reductase, RubisCO). The enrichment of citrate cycle-related modules at the DCM in the cyclone and at 150 m depth in the anticyclone indicates that the apparent increases in phototrophic metabolism that occurred at these eddy sites and depths were followed by increases in cellular respiration and ATP synthesis.

CONCLUSION

This study provides insight as to how changes in the physiochemical environment that result from mesoscale eddy activity may alter protistan community structure and function in the oligotrophic ocean. The results of the metatranscriptomic analysis revealed that many of the taxonomic and metabolic differences observed between protistan communities in eddies of opposite polarity were noted at and below the DCM and likely resulted from eddy-induced vertical shifts in the water column. Specifically, the metatranscriptomes collected in this study demonstrated that protistan communities at 150 m depth in the anticyclone were taxonomically and metabolically more similar to DCM communities than were the protistan communities at 150 m depth in the cyclone. Differences in the abundances of phototrophy- and heterotrophy-associated transcripts for all eukaryotes and for specific protistan taxa at 150 m depth further highlighted the potential role that mesoscale eddies play in influencing the metabolism and nutritional physiology of protists at the base of the euphotic zone. These observations suggest that mesoscale eddies can alter the depth at which organic carbon is fixed, repackaged, redistributed, and remineralised by marine protists and can therefore alter the amount of carbon that is exported out of the euphotic zone.

AUTHOR CONTRIBUTIONS

Samantha J. Gleich: Conceptualization; data curation; formal analysis; visualization; writing – original draft; writing – review and editing. **Sarah Hu:** Formal analysis; writing – original draft; writing – review and editing. **Arianna I. Krinos:** Formal analysis; writing – review and editing; writing – original draft. **David A. Caron:** Conceptualization; funding acquisition; writing – original draft; writing – review and editing.

ACKNOWLEDGEMENTS

We are grateful to Tara Clemente and Timothy Burrell for collecting the metatranscriptomic samples that were analysed in this study during the 2018 FALKOR cruise. We would also like to thank all of the scientists and crew members who contributed to the 2018 FALKOR cruise activities and the Schmidt Ocean Institute for funding the FALKOR cruise ship time. This work and SJG were supported by the Simons Collaboration on Ocean Processes and Ecology (P49802 to DAC). SKH was supported by NSF award OCE-2327203. AIK was supported by the Department of Energy Computational Science Graduate Fellowship (DE-SC0020347 to AIK) and by the Simons Collaboration on Computational Biogeochemical Modelling of Marine Ecosystems (CBIOMES) (grant no. 549931).

CONFLICT OF INTEREST STATEMENT

The authors declare that they have no conflict of interest.

DATA AVAILABILITY STATEMENT

Raw sequence data associated with this project are available on NCBI under accession number PRJNA982163: https://www.ncbi.nlm.nih.gov/bioproject/PRJNA982163. The bioinformatics pipeline and the scripts used to process and analyze the sequence data are available on GitHub: https://github.com/sgleich/FalkorMetaT.

ORCID

Samantha J. Gleich https://orcid.org/0000-0002-4613-7171

REFERENCES

Allen, A. (2015) *PhyloDB*. GitHub: GitHub repository. http://github.com/allenlab/PhyloDB

Armstrong, F.A.J., Sterns, C.R. & Strickland, J.D.H. (1967) The measurement of upwelling and subsequent biological processes by means of the Technicon autoanalyzer and associated equipment. *Deep Sea Research*, 14, 381–389.

Barone, B., Church, M.J., Dugenne, M., Hawco, N.J., Jahn, O., White, A.E. et al. (2022) Biogeochemical dynamics in adjacent mesoscale eddies of opposite polarity. *Global Biogeochemical Cycles*, 36(2), e2021GB007115.

Barone, B., Coenen, A.R., Beckett, S.J., McGillicuddy, D.J., Weitz, J.S. & Karl, D.M. (2019) The ecological and biogeochemical state of the North Pacific Subtropical Gyre is linked to sea surface height. *Journal of Marine Research*, 77, 215–245.

Becker, K.W., Harke, M.J., Mende, D.R., Muratore, D., Weitz, J.S., DeLong, E.F. et al. (2021) Combined pigment and metatranscriptomic analysis reveals highly synchronized diel patterns of phenotypic light response across domains in the open oligotrophic ocean. *The ISME Journal*, 15, 520–533.

Belkin, N., Guy-Haim, T., Rubin-Blum, M., Lazar, A., Sisma-Ventura, G., Kiko, R. et al. (2022) Influence of cyclonic and anticyclonic eddies on phytoplankton biomass, activity and diversity in the southeastern Mediterranean Sea. *Ocean Science*, 18, 693–715.

Bender, S.J., Durkin, C.A., Berthiaume, C.T., Morales, R.L. & Armbrust, E.V. (2014) Transcriptional responses of three model diatoms to nitrate limitation of growth. *Frontiers in Marine Science*, 1, 3.

Benitez-Nelson, C.R., Bidigare, R.R., Dickey, T.D., Landry, M.R., Leonard, C.L., Brown, S.L. et al. (2007) Mesoscale eddies drive increased silica export in the subtropical Pacific Ocean. *Science*, 316, 1017–1021.

Berg, G.M., Shrager, J., Glöckner, G., Arrigo, K.R. & Grossman, A.R. (2008) Understanding nitrogen limitation in *Aureococcus anophagefferens* (Pelagophyceae) through cDNA and qRT-PCR analysis. *Journal of Phycology*, 44, 1235–1249.

Bidigare, R.R., Benitez-Nelson, C., Leonard, C.L., Quay, P.D., Parsons, M.L., Foley, D.G. et al. (2003) Influence of a cyclonic eddy on microheterotroph biomass and carbon export in the lee of Hawaii. *Geophysical Research Letters*, 30(6), 51.

Boeuf, D., Edwards, B.R., Eppley, J.M., Hu, S.K., Poff, K.E., Romano, A.E. et al. (2019) Biological composition and microbial dynamics of sinking particulate organic matter at abyssal depths in the oligotrophic open ocean. *Proceedings of the National Academy of Sciences of the United States of America*, 116(24), 11824–11832.

Bolger, A.M., Lohse, M. & Usadel, B. (2014) Trimmomatic: a flexible trimmer for Illumina sequence data. *Bioinformatics*, 30(15), 2114–2120.

Boyle, E.I., Weng, S., Gollub, J., Jin, H., Botstein, D., Cherry, J.M. et al. (2004) GO::TermFinder—open source software for accessing Gene Ontology information and finding significantly enriched Gene Ontology terms associated with a list of genes. *Bioinformatics*, 20(18), 3710–3715.

Bracco, A., Provenzale, A. & Scheuring, I. (2000) Mesoscale vortices and the paradox of the plankton. *Proceedings of the Royal Society of London. Series B, Biological Sciences*, 267(1454), 1795–1800.

Brown, S.L., Landry, M.R., Selph, K.E., Yang, E.J., Rii, Y.M. & Bidigare, R.R. (2008) Diatoms in the desert: plankton community response to a mesoscale eddy in the subtropical North Pacific. *Deep-Sea Research Part II: Topical Studies in Oceanography*, 55(10-13), 1321–1333.

Buck, K.R., Marin, R., III & Chavez, F.P. (2005) Heterotrophic dinoflagellate fecal pellet production: grazing of large, chain-forming diatoms during upwelling events in Monterey Bay, California. *Aquatic Microbial Ecology*, 40, 293–298.

Buesseler, K.O., Lamborg, C., Cai, P., Escoube, R., Johnson, R., Pike, S. et al. (2008) Particle fluxes associated with mesoscale eddies in the Sargasso Sea. *Deep-Sea Research Part II: Topical Studies in Oceanography*, 55, 1426–1444.

Burns, J.A., Pittis, A.A. & Kim, E. (2018) Gene-based predictive models of trophic modes suggest Asgard archaea are not phagocytotic. *Nature Ecology & Evolution*, 2, 697–704.

Calbet, A. & Landry, M.R. (2004) Phytoplankton growth, microzooplankton grazing, and carbon cycling in marine systems. *Limnology and Oceanography*, 49(1), 51–57.

Caporaso, J.G., Kuczynski, J., Stombaugh, J., Bittinger, K., Bushman, F.D., Costello, E.K. et al. (2010) QIIME allows analysis of high-throughput community sequencing data. *Nature Methods*, 7, 335–336.

Caron, D.A., Countway, P.D., Jones, A.C., Kim, D.Y. & Schnetzer, A. (2012) Marine protistan diversity. *Annual Review of Marine Science*, 4, 467–493.

Chelton, D.B., Schlax, M.G. & Samelson, R.M. (2011) Global observations of nonlinear mesoscale eddies. *Progress in Oceanography*, 91(2), 167–216.

Church, M.J., Mahaffey, C., Letelier, R.M., Lukas, R., Zehr, J.P. & Karl, D.M. (2009) Physical forcing of nitrogen fixation and diazotroph community structure in the North Pacific Subtropical Gyre. *Global Biogeochemical Cycles*, 23, GB2020.

Cohen, N.R., McIlvin, M.R., Moran, D.W., Held, N.A., Saunders, J.K., Hawco, N.J. et al. (2021) Dinoflagellates alter their carbon and nutrient metabolic strategies across environmental gradients in the Central Pacific Ocean. *Nature Microbiology*, 6, 173–186.

Cornec, M., Laxenaire, R., Speich, S. & Claustre, H. (2021) Impact of mesoscale eddies on deep chlorophyll maxima. *Geophysical Research Letters*, 48, e2021GL093470.

Cotti-Rausch, B.E., Lomas, M.W., Lachenmyer, E.M., Goldman, E.A., Bell, D.W., Goldberg, S.R. et al. (2016) Mesoscale and submesoscale variability in phytoplankton community composition in the Sargasso Sea. *Deep-Sea Research Part I: Oceanographic Research Papers*, 110, 106–122.

Décima, M. & Landry, M.R. (2020) Resilience of plankton trophic structure to an eddy-stimulated diatom bloom in the North Pacific Subtropical Gyre. *Marine Ecology Progress Series*, 643, 33–48.

Dugenne, M., Gradoville, M.R., Church, M.J., Wilson, S.T., Sheyn, U., Harke, M.J. et al. (2023) Nitrogen fixation in mesoscale eddies of the North Pacific Subtropical Gyre: patterns and mechanisms. *Global Biogeochemical Cycles*, 37(4), e2022GB007386.

Emms, D.M. & Kelly, S. (2019) OrthoFinder: phylogenetic ortohlogy inference for comparative genomics. *Genome Biology*, 20, 238.

Falkowski, P.G., Ziemann, D., Kolber, Z. & Bienfang, P.K. (1991) Role of eddy pumping in enhancing primary production in the ocean. *Nature*, 352, 55–58.

Fong, A.A., Karl, D.M., Lukas, R., Letelier, R.M., Zehr, J.P. & Church, M.J. (2008) Nitrogen fixation in an anticyclonic eddy in the oligotrophic North Pacific Ocean. *The ISME Journal*, 2, 663–676.

Gaston, D. & Roger, A.J. (2013) Functional divergence and convergent evolution in the plastid-targeted glyceraldehyde-3-phosphate dehydrogenases of diverse eukaryotic algae. *PLoS One*, 8(7), e70396.

Giner, C.R., Pernice, M.C., Balagué, V., Duarte, C.M., Gasol, J.M., Logares, R. et al. (2020) Marked changes in diversity and relative activity of picoeukaryotes with depth in the world ocean. *The ISME Journal*, 14, 437–449.

Grabherr, M.G., Haas, B.J., Yassour, M., Levin, J.Z., Thompson, D.A., Ammit, I. et al. (2011) Full-length transcriptome assembly from RNA-seq data without a reference genome. *Nature Biotechnology*, 29(7), 644–654.

Guidi, L., Calil, P.H.R., Duhamel, S., Björkman, K.M., Doney, S.C., Jackson, G.A. et al. (2012) Does eddy-eddy interaction control surface phytoplankton distribution and carbon export in the North Pacific Subtropical Gyre? *Journal of Geophysical Research*, 117, G02024.

Guillou, L., Bachar, D., Audic, S., Bass, D., Berney, C., Bittner, L. et al. (2013) The protist ribosomal reference database (PR2): a catalog of unicellular eukaryote small sub-unit rRNA sequences with curated taxonomy. *Nucleic Acids Research*, 41, D597–D604.

Hansen, P.J. (2011) The role of photosynthesis and food uptake for the growth of marine mixotrophic dinoflagellates. *The Journal of Eukaryotic Microbiology*, 58(3), 203–214.

Harke, M.J., Frischkorn, K.R., Hennon, G.M.M., Haley, S.T., Barone, B., Karl, D.M. et al. (2021) Microbial community transcriptional patterns vary in response to mesoscale forcing in the North Pacific Subtropical Gyre. *Environmental Microbiology*, 23(8), 4807–4822.

Hu, S.K., Liu, Z., Alexander, H., Campbell, V., Connell, P.E., Dyhrman, S.T. et al. (2018) Shifting metabolic priorities among key protistan taxa within and below the euphotic zone. *Environmental Microbiology*, 20(8), 2865–2879.

Huang, J., Xu, F., Zhou, K., Xiu, P. & Lin, Y. (2017) Temporal evolution of near-surface chlorophyll over cyclonic eddy lifecycles in the southeastern Pacific. *Journal of Geophysical Research, Oceans*, 122, 6165–6179.

Huerta-Cepas, J., Forslund, K., Coelho, L.P., Szklarczyk, D., Jensen, L.J., von Mering, C. et al. (2017) Fast genome-wide functional annotation through orthology assignment by eggnog-mapper. *Molecular Biology and Evolution*, 34(8), 2115–2122.

Huerta-Cepas, J., Szklarczyk, D., Heller, D., Hernández-Plaza, A., Forslund, S.K., Cook, H. et al. (2019) Eggnog 5.0: a hierarchical, functionally and phylogenetically annotated orthology resource based on 5090 organisms and 2502 viruses. *Nucleic Acids Research*, 47(D1), D309–D314.

Jacobson, D.M. & Anderson, D.M. (1986) Thecate heterotrophic dinoflagellates: feeding behavior and mechanisms. *Journal of Phycology*, 22, 249–258.

Jeong, H.J., Yoo, Y.D., Kim, J.E., Kim, T.H., Kim, J.H., Kang, N.S. et al. (2004) Mixotrophy in the phototrophic harmful alga *Cochlodinium polykrikoides* (Dinophycean): prey species, the effects of prey concentration, and grazing impact. *The Journal of Eukaryotic Microbiology*, 51(5), 563–569.

Jeong, H.J., Yoo, Y.D., Kim, J.S., Seong, K.A., Kang, N.S. & Kim, T.H. (2010) Growth, feeding and ecological roles of the mixotrophic and heterotrophic dinoflagellates in marine planktonic food webs. *Ocean Science Journal*, 45, 65–91.

Karl, D.M. (1999) A sea of change: biogeochemical variability in the North Pacific Subtropical Gyre. *Ecosystems*, 2, 181–214.

Karl, D.M., Christian, J.R., Dore, J.E., Hebel, D.V., Letelier, R.M., Tupas, L.M. et al. (1996) Seasonal and interannual variability in primary production and particle flux at station ALOHA. *Deep-Sea Research Part II: Topical Studies in Oceanography*, 43(2-3), 539–568.

Karl, D.M. & Church, M.J. (2017) Ecosystem structure and dynamics in the North Pacific Subtropical Gyre: new views of an old ocean. *Ecosystems*, 20, 433–457.

Kazamia, E., Sutak, R., Paz-Yepes, J., Dorrell, R.G., Rocha Jimenez Vieira, F., Mach, J. et al. (2018) Endocytosis-mediated siderophore uptake as a strategy for Fe acquisition in diatoms. *Science Advances*, 4, eaar4536.

Klemetsen, T., Raknes, I.A., Agafonov, A., Balasundaram, S.V., Tartari, G., Robertsen, E. et al. (2018) The MAR databases: development and implementation of databases specific for marine metagenomics. *Nucleic Acids Research*, 4(46), D692–D699.

Koppelle, S., López-Escardó, D., Brussaard, C.P.D., Philippart, C.J.M., Massana, R. & Wilken, S. (2022) Mixotrophy in the bloom-forming genus *Phaeocystis* and other haptophytes. *Harmful Algae*, 117, 102292.

Kopylova, E., Noé, L. & Touzet, H. (2012) SortMeRNA: fast and accurate filtering of ribosomal RNAs in metatranscriptomic data. *Bioinformatics*, 28(24), 3211–3217.

Krinos, A.I., Hu, S.K., Cohen, N.R. & Alexander, H. (2021) EUKulele: taxonomic annotation of the unsung eukaryotic microbes. *Journal of Open Source Software*, 5(54), 2799.

Labarre, A., Obiol, A., Wilken, S., Forn, I. & Massana, R. (2020) Expression of genes involved in phagocytosis in uncultured heterotrophic flagellates. *Limnology and Oceanography*, 65, S149–S160.

Lambert, B.S., Groussman, R.D., Schatz, M.J., Coesel, S.N., Durham, B.P., Alverson, A.J. et al. (2022) The dynamic trophic architecture of open-ocean protist communities revealed through machine-guided metatranscriptomics. *PNAS*, 119(7), e2100916119.

Landry, M.R., Brown, S.L., Rii, Y.M., Selph, K.E., Bidigare, R.R., Yang, E.J. et al. (2008) Depth-stratified phytoplankton dynamics in cyclone opal, a subtropical mesoscale eddy. *Deep-Sea Research Part II: Topical Studies in Oceanography*, 55, 1348–1359.

Letelier, R.M., Karl, D.M., Abbott, M.R., Flament, P., Freilich, M., Lukas, R. et al. (2000) Role of late winter mesoscale events in the biogeochemical variability of the upper water column of the North Pacific Subtropical Gyre. *Journal of Geophysical Research*, 105(C12), 723–739.

Li, D., Liu, C.M., Luo, R., Sadakane, K. & Lam, T.W. (2015) MEGAHIT: an ultra-fast single-node solution for large and complex metagenomics assembly via succinct de Bruijn graph. *Bioinformatics*, 31(10), 1674–1676.

Lie, A.A.Y., Liu, Z., Terrado, R., Tatters, A.O., Heidelbebrg, K.B. & Caron, D.A. (2017) Effect of light and prey availability on gene

expression of the mixotrophic chrysophyte, *Ochromonas* sp. *BMC Genomics*, 18, 163.

Liu, Z., Campbell, V., Heidelberg, K.B. & Caron, D.A. (2016) Gene expression characterizes different nutritional strategies among three mixotrophic protists. *FEMS Microbiology Ecology*, 92(7), fiw106.

Liu, Z., Jones, A.C., Campbell, V., Hambright, K.D., Heidelberg, K.B. & Caron, D.A. (2015) Gene expression in the mixotrophic prymnesiophyte, *Prymnesium parvum*, responds to prey availability. *Frontiers in Microbiology*, 6, 319.

Lund, S.P., Nettleton, D., McCarthy, D.J. & Smyth, G.K. (2012) Detecting differential expression in RNA-sequence data using quasi-likelihood with shrunken dispersion estimates. *Statistical Applications in Genetics and Molecular Biology*, 11(5), 8.

Maiti, K., Benitez-Nelson, C.R., Rii, Y. & Bidigare, R. (2008) The influence of a mature cyclonic eddy on particle export in the lee of Hawaii. *Deep-Sea Research Part II: Topical Studies in Oceanography*, 55, 1445–1460.

Massana, R., Labarre, A., López-Escardó, D., Obiol, A., Bucchini, F., Hackl, T. et al. (2021) Gene expression during bacterivorous growth of a widespread marine heterotrophic flagellate. *The ISME Journal*, 15, 154–167.

McGillicuddy, D.J. (2016) Mechanisms of physical-biological-biogeochemical interaction at the oceanic mesoscale. *Annual Review of Marine Science*, 8, 125–159.

McGillicuddy, D.J., Anderson, L.A., Bates, N.R., Bibby, T., Buesseler, K.O., Carlson, C.A. et al. (2007) Eddy/wind interactions simulate extraordinary mid-ocean plankton blooms. *Science*, 316, 1021–1026.

McGillicuddy, D.J., Robinson, A.R., Siegel, D.A., Jannasch, H.W., Dickey, T.D., McNeil, J. et al. (1998) Influence of mesoscale eddies on new production in the Sargasso Sea. *Nature*, 394, 263–266.

McKie-Krisberg, Z.M., Sanders, R.W. & Gast, R.J. (2018) Evaluation of mixotrophy-associated gene expression in two species of polar marine algae. *Frontiers in Marine Science*, 5, 273.

Monger, B.C. & Landry, M.R. (1993) Flow cytometric analysis of marine bacteria with Hoechst 33342. *Applied and Environmental Microbiology*, 59, 905–911.

Murphy, J. & Riley, J.P. (1962) A modified single solution method for the determination of phosphate in natural waters. *Analytica Chimica Acta*, 27, 31–36.

Nelson, C.E., Carlson, C.A., Ewart, C.S. & Halewood, E.R. (2014) Community differentiation and population enrichment of Sargasso Sea bacterioplankton in the euphotic zone of a mesoscale mode-water eddy. *Environmental Microbiology*, 16(3), 871–887.

Nencioli, F., Kuwahara, V.S., Dickey, T.D., Rii, Y.M. & Bidigare, R.R. (2008) Physical dynamics and biological implications of a mesoscale eddy in the lee of Hawai'i: cyclone *Opal* observations during E-flux III. *Deep-Sea Research Part II: Topical Studies in Oceanography*, 55, 1252–1274.

Obiol, A., López-Escardó, D., Salomaki, E.D., Wiśniewski, M.M., Forn, I., Sà, E. et al. (2023) Gene expression dynamics of natural assemblages of heterotrophic flagellates during bacterivory. *Microbiome*, 11, 134.

Ollison, G.A., Hu, S.K., Mesrop, L.Y., DeLong, E.F. & Caron, D.A. (2021) Come rain or shine: depth not season shapes the active protistan community at station ALOHA in the North Pacific Subtropical Gyre. *Deep-Sea Research Part I: Oceanographic Research Papers*, 170, 103494.

Paterson, H.L., Knott, B. & Waite, A.M. (2007) Microzooplankton community structure and grazing on phytoplankton, in an eddy pair in the Indian Ocean off Western Australia. *Deep-Sea Research Part II: Topical Studies in Oceanography*, 54, 1076–1093.

Patro, R., Duggal, G., Love, M.I., Irizarry, R.A. & Kingsford, C. (2017) Salmon provides fast and bias-aware quantification of transcript expression. *Nature Methods*, 14(4), 417–419.

Poff, K.E., Leu, A.O., Eppley, J.M., Karl, D.M. & DeLong, E.F. (2021) Microbial dynamics of elevated carbon flux in the open ocean's abyss. *PNAS*, 118(4), e2018269118.

R Core Team. (2022) *R: a language and environment for statistical computing*. Vienna, Austria: R Foundation for Statistical Computing.

Rii, Y.M., Brown, S.L., Nencioli, F., Kuwahra, V., Dickey, T., Karl, D.M. et al. (2008) The transient oasis: nutrient-phytoplankton dynamics and particle export in Hawaiian lee cyclones. *Deep-Sea Research Part II: Topical Studies in Oceanography*, 55(10-13), 1275–1290.

Rii, Y.M., Peoples, L.M., Karl, D.M. & Church, M.J. (2022) Seasonality and episodic variation in picoeukaryotic diversity and structure reveal community resilience to disturbances in the North Pacific Subtropical Gyre. *Limnology and Oceanography*, 67, S331–S351.

Robinson, M.D., McCarthy, D.J., & Smyth, G.K. (2010) edgeR: a Bioconductor package for differential expression analysis of digital gene expression dataedgeR: a Bioconductor package for differential expression analysis of digital gene expression data. *Bioinformatics*, 26(1), 139–140.

Rogers, M. & Keeling, P.J. (2004) Lateral transfer and recompartmentalization of Calvin cycle enzymes of plants and algae. *Journal of Molecular Evolution*, 58, 367–375.

Rubin, E.T., Cheng, S., Montalbano, A.L., Menden-Deuer, S. & Rynearson, T.A. (2019) Transcriptomic response to feeding and starvation in a herbivorous dinoflagellate. *Frontiers in Marine Science*, 6, 246.

Santoferrara, L.F., Guida, S., Zhang, H. & McManus, G.B. (2014) De novo transcriptomes of a mixotrophic and a heterotrophic ciliate from marine plankton. *PLoS One*, 9(7), e101418.

Sherr, E.B. & Sherr, B.F. (1994) Bacterivory and herbivory: key roles of phagotrophic protists in pelagic food webs. *Microbial Ecology*, 28, 223–235.

Sherr, E.B. & Sherr, B.F. (2007) Heterotrophic dinoflagellates: a significant component of microzooplankton biomass and major grazers of diatoms in the sea. *Marine Ecology Progress Series*, 352, 187–197.

Shim, J., Klochkova, T.A., Han, J.W., Kim, G.H., Yoo, Y.D. & Jeong, H.J. (2011) Comparative proteomics of the mixotrophic dinoflagellate *Prorocentrum micans* growing in different trophic modes. *Algae*, 26(1), 87–96.

Siegel, D.A., Court, D.B., Menzies, D.W., Peterson, P., Maritoreng, S. & Nelson, N.B. (2008) Satellite and in situ observations of the bio-optical signatures of two mesoscales eddies in the Sargasso Sea. *Deep-Sea Research Part II: Topical Studies in Oceanography*, 55(10–13), 1218–1230.

Steinberg, D.K. & Landry, M.R. (2017) Zooplankton and the ocean carbon cycle. *Annual Review of Marine Science*, 9, 413–444.

Steinegger, M. & Söding, J. (2018) Clustering huge protein sequence sets in linear time. *Nature Communications*, 9, 2542.

Stoecker, D.K. (1998) Conceptual models of mixotrophy in planktonic protists and some ecological and evolutionary implications. *European Journal of Protistology*, 34, 281–290.

Stoecker, D.K., Hansen, P.J., Caron, D.A. & Mitra, A. (2017) Mixotrophy in the marine plankton. *Annual Review of Marine Science*, 9, 311–335.

Sukigara, C., Suga, T., Toyama, K. & Oka, E. (2014) Biogeochemical responses associated with the passage of a cyclonic eddy based on shipboard observations in the western North Pacific. *Journal of Oceanography*, 70, 435–445.

Suttle, C.A., Chan, A.M., Taylor, W.D. & Harrison, P.J. (1986) Grazing of planktonic diatoms by microflagellates. *Journal of Plankton Research*, 8(2), 393–398.

Tang, S., Lomsadze, A. & Borodovsky, M. (2015) Identification of protein coding regions in RNA transcripts. *Nucleic Acids Research*, 43(12), e78.

Vaillancourt, R.D., Marra, J., Seki, M.P., Parsons, M.L. & Bidigare, R.R. (2003) Impact of a cyclonic eddy on phytoplankton community structure and photosynthetic competency in the subtropical North Pacific Ocean. *Deep-Sea Research Part I: Oceanographic Research Paper*, 50(7), 829–847.

Venkatachalam, S., Ansorge, I.J., Mendes, A., Melato, L.I., Matcher, G.F. & Dorrington, R.A. (2017) A pivotal role for ocean eddies in the distribution of microbial communities across the Antarctic circumpolar current. *PLoS One*, 12(8), e0183400.

Ward, B.A. (2019) Mixotroph ecology: more than the sum of its parts. *PNAS*, 116(13), 1902106116.

Wear, E.K., Carlson, C.A. & Church, M.J. (2020) Bacterioplankton metabolism of phytoplankton lysates across a cyclone-anticyclone eddy dipole impacts the cycling of semi-labile organic matter in the photic zone. *Limnology and Oceanography*, 65, 1608–1622.

Wijesooriya, K., Jadaan, S.A., Perera, K.L., Kaur, T. & Ziemann, M. (2022) Urgent need for consistent standards in functional enrichment analysis. *PLoS Computational Biology*, 18(3), e1009935.

Worden, A.Z., Follows, M.J., Giovannoni, S.J., Wilken, S., Zimmerman, A.E. & Keeling, P.J. (2015) Rethinking the marine carbon cycle: factoring in the multifarious lifestyles of microbes. *Science*, 347(6223), 1257594.

Wu, T., Hu, E., Xu, S., Chen, M., Guo, P., Dai, Z. et al. (2021) clusterProfiler 4.0: a universal enrichment tool for interpreting omics data. *Innovation*, 2(3), 100141.

Xiu, P. & Chai, F. (2020) Eddies affect subsurface phytoplankton and oxygen distributions in the North Pacific Subtropical Gyre. *Geophysical Research Letters*, 47, e2020GL087037.

Yee, D.P., Hildebrand, M. & Tresguerres, M. (2019) Dynamic subcellular translocation of V-type H+-ATPase is essential for biomineralization of the diatom silica cell wall. *The New Phytologist*, 225, 2411–2422.

Yutin, N., Wolf, M.Y., Wolf, Y.I. & Koonin, E.V. (2009) The origins of phagocytosis and eukaryogenesis. *Biology Direct*, 4, 9.

Zhou, K., Benitez-Nelson, C.R., Huang, J., Sun, Z. & Dai, M. (2021) Cyclonic eddies modulate temporal and spatial decoupling of particulate carbon, nitrogen, and biogenic silica export in the North Pacific Subtropical Gyre. *Limnology and Oceanography*, 66, 3508–3522.

SUPPORTING INFORMATION

Additional supporting information can be found online in the Supporting Information section at the end of this article.

How to cite this article: Gleich, S.J., Hu, S.K., Krinos, A.I. & Caron, D.A. (2024) Protistan community composition and metabolism in the North Pacific Subtropical Gyre: Influences of mesoscale eddies and depth. *Environmental Microbiology*, 26(1), e16556. Available from: https://doi.org/10.1111/1462-2920.16556